Published online 4 November 2022 *Nucleic Acids Research, 2022, Vol. 50, No. 20* **11529–11549**
https://doi.org/10.1093/nar/gkac980

eIF3j inhibits translation of a subset of circular RNAs in eukaryotic cells

Zhenxing Song[1,†], Jiamei Lin[1,†], Rui Su[1], Yu Ji[1], Ruirui Jia[1], Shi Li[1], Ge Shan[2] and Chuan Huang[1,*]

[1]School of Life Sciences, Chongqing University, Chongqing 401331, China and [2]School of Basic Medical Sciences, Division of Life Science and Medicine, University of Science and Technology of China, Hefei 230027, China

Received September 12, 2022; Revised October 04, 2022; Editorial Decision October 05, 2022; Accepted October 17, 2022

ABSTRACT

Increasing studies have revealed that a subset of circular RNAs (circRNAs) harbor an open reading frame and can act as protein-coding templates to generate functional proteins that are closely associated with multiple physiological and disease-relevant processes, and thus proper regulation of synthesis of these circRNA-derived proteins is a fundamental cellular process required for homeostasis maintenance. However, how circRNA translation initiation is coordinated by different *trans*-acting factors remains poorly understood. In particular, the impact of different eukaryotic translation initiation factors (eIFs) on circRNA translation and the physiological relevance of this distinct regulation have not yet been characterized. In this study, we screened all 43 *Drosophila* eIFs and revealed the conflicting functions of eIF3 subunits in the translational control of the translatable circRNA *circSfl*: eIF3 is indispensable for *circSfl* translation, while the eIF3-associated factor eIF3j is the most potent inhibitor. Mechanistically, the binding of eIF3j to *circSfl* promotes the disassociation of eIF3. The C-terminus of eIF3j and an RNA regulon within the *circSfl* untranslated region (UTR) are essential for the inhibitory effect of eIF3j. Moreover, we revealed the physiological relevance of eIF3j-mediated *circSfl* translation repression in response to heat shock. Finally, additional translatable circRNAs were identified to be similarly regulated in an eIF3j-dependent manner. Altogether, our study provides a significant insight into the field of cap-independent translational regulation and undiscovered functions of eIF3.

INTRODUCTION

Circular RNA (circRNA) is a class of covalently closed RNA molecules discovered in diverse species (1–4). A small amount of circRNAs are outputs of non-coding regions (e.g. intronic circRNAs) (5–8), whereas the majority of circRNAs are generated from one or multiple exons of eukaryotic protein-coding genes via back-splicing, by which a splicing donor joins an upstream splicing acceptor (9–12). Due to lacking of canonical features that are usually utilized by linear RNAs, the regulation of circRNAs is distinct from that of their linear counterparts. Take nuclear export as an example. Once generated, linear mRNAs are typically capped at the 5′ end and polyadenylated at the 3′ end. A subset of export adaptors can recognize RNA cargoes as/with cap- or poly (A)-binding proteins and establish a physical bridge for linear mRNAs and their export receptors (13,14). Since circRNAs have no free ends, they must be exported via a different mechanism. In support, our recent study has demonstrated that the evolutionarily conserved receptor Exportin-4 (XPO4) directly binds to a subset of circRNAs, but not their linear counterparts, to facilitate their nuclear export (15).

Perturbations in circRNA expression are closely associated with cellular physiology and many diseases (16–20). A plenty of circRNAs have been demonstrated to directly regulate various physiological or pathological processes through diverse mechanisms, such as sponging microRNAs, forming DNA-RNA hybrids (R-loops), and interacting with RNA binding proteins (RBPs) (21–26). For example, *circTLK1*, an ischemic stroke-associated circRNA, can sequester *miR-335-3p* away from its target *TIPARP*, pathologically aggravating brain infarction and neuronal injury (25). *CircSMARCA5* blocks *SMARCA5* transcription via an R-loop structure formed at exons 15–16 in breast cancer cells (26). *CircNSUN2* recruits the RBP IGF2BP2 to enhance the stability of *HMGA2* mRNA, which results in an increased level of HMGA2 protein that promotes colorectal liver metastasis (24).

*To whom correspondence should be addressed. Tel: +86 19956025374; Email: chuanhuang@cqu.edu.cn
†The authors wish it to be known that, in their opinion, the first two authors should be regarded as Joint First Authors.

Although it was long assumed that circRNA is a type of non-coding RNAs without translation ability, emerging studies have demonstrated that a subgroup of endogenous circRNAs are bound by polyribosomes and the translation of circRNAs may be pervasive in eukaryotes (27–30). Moreover, circRNAs have been found to exert physiological or molecular roles through their encoded proteins in recent years (31–33). For example, the insulin-sensitive circRNA *circSfl* shares the start codon with its linear counterpart and encodes a truncated sulfateless (Sfl) protein which contributes to the lifespan extension of fruit flies (34). *CircE-Cad*-derived C-E-Cad protein maintains the tumorigenicity of glioma stem cells by activing an array of cancer-relevant pathways, such as STAT3, PI3K-AKT and MAPK-ERK signaling (35). Additionally, a circRNA generated from the long non-coding RNA *LINC-PINT* is capable of encoding a tumor-suppressive protein which regulates the transcriptional elongation of oncogenes in glioblastoma (7). These studies suggest that circRNA-derived proteins represent essential regulators in normal physiology and multiple diseases, and that the proper regulation of circRNA translation is required for cellular homeostasis maintenance. In fact, some RNA regulons, including internal ribosomal entry site (IRES)-like and m^6A-modified elements, have been implicated as *cis*-acting factors to initiate circRNA translation (27–29). However, what *trans*-acting eukaryotic translation initiation factors (eIFs) function in the translation initiation of circRNAs is still poorly understood.

In eukaryotic cells, eIF3 is a multi-subunit complex containing 12 subunits and consists of two interconnected modules which are assembled by the nucleation core eIF3a and eIF3b (36–38). eIF3 plays essential roles in several steps of translation initiation of linear mRNAs, such as 43S pre-initiation complex (PIC) assembly, mRNA recruitment to the 43S PIC, and start codon recognition/selection (36–38). Beyond its canonical roles, eIF3 has also been implicated as an inhibitor in the translation of certain stress-responsive and proliferation-relevant mRNAs, such as *FTL* and *BTG1* (39,40). Moreover, eIF3 can recognize 5′ end of specific mRNAs and promote initiation complex formation in an eIF4E-independent manner (41). Although eIF3j was first thought to represent the 13th subunit of eIF3, emerging evidence supports that it often functions in an eIF3-independent manner and is not a *bona fide* eIF3 subunit (36–38).

Using a model translatable circRNA (*Drosophila circSfl*), we here evaluated the impact of all 43 *Drosophila* eIFs on circRNA translation by a systematic RNAi screening. The eIF3 complex was found to promote the translation efficiency of *circSfl*, while eIF3j was identified as the most potent inhibitor. Mechanistically, eIF3j induces translation repression by promoting the disassociation of the eIF3 complex from *circSfl*. The binding of eIF3j to circRNA templates requires its C-terminus and is essential for the inhibitory activity of eIF3j. Moreover, we demonstrated an RNA regulon within the *circSfl* untranslated region (UTR) that facilitates eIF3j recruitment and, in turn, translation repression, supporting a combinatorial control of circRNA translation initiation by *cis*-regulatory RNA elements and *trans*-regulatory protein factors. In addition, we revealed that eIF3j negatively regulates the heat resistance of *circSfl*-enriched cells by attenuating *circSfl* translation in cellular response to heat stress, suggesting a stress-responsive mechanism to ensure clean of damaged cells. Finally, we identified additional translatable circRNAs whose translation is similarly regulated by eIF3j. Focused studies on *circPde8* confirmed the general role of eIF3j in circRNA translation. Altogether, our findings provide an insight into the previously undiscovered eIF3j-mediated circRNA translational control and illustrate the physiological relevance of this distinct regulation.

MATERIALS AND METHODS

Cell culture and stable cell line construction

Drosophila Schneider 2 (S2) cells were grown in Schneider's *Drosophila* medium (Sigma, S9895) supplemented with 10% fetal bovine serum (v/v; HyClone, SH30910.03) and 1% penicillin streptomycin (v/v; Thermo Fisher Scientific, 15140122) at 25°C. To generate a stable cell line, 1.0×10^6 S2 cells in a well of the 12-well plate were transfected with 1 μg of the indicated plasmid (Supplementary Plasmid Information) using Lipo6000 (Beyotime, C0526) for 3 days according to the manufacturer's protocol. The transfected cells were then transferred to fresh medium and maintained by selection with 150 μg/ml hygromycin B (Biofroxx, 1366ML010) for another 3–4 weeks.

Plasmids and cloning

All plasmids used in this study were generated by modifying the Hy_pMT EGFP SV40 pA plasmid (Addgene, #69911), in which the *copia* transposon LTR promoter drives *HygroR* transcription and the *MtnA* promoter (a copper-inducible promoter) drives *EGFP* transcription (42). All cloning details are provided in Supplementary Plasmid Information.

Double-stranded RNA preparation

The detailed information of each double-stranded RNA (dsRNA) used in this study is provided in Supplementary Table S1. DNA templates of dsRNAs were prepared by PCR reactions with primer pairs containing the T7 promoter sequence (TAATACGACTCACTATAGGG) on the 5′ end. DsRNAs were then generated by *in vitro* transcription using ScriptMAX® Thermo T7 Transcription Kit (TOYOBO, TSK-101) according to the manufacturer's protocol.

RNAi and ASO directed knockdown

For dsRNA bathing, a total of 1.5×10^6 S2 cells were suspended in 600 μl of serum-free medium containing 8 μg of the indicated dsRNA for 30 min. 400 μl of medium containing 20% fetal bovine serum (v/v) was then added and cells were maintained for 3 days at 25°C. For small interfering RNA (siRNA) or antisense oligonucleotide (ASO) transfection, a total of 1.5×10^6 S2 cells were transfected with the indicated siRNA (final concentration: 80 nM) or ASO (final concentration: 50 nM) for 2 days using Lipofectamine® RNAiMAX Reagent (Invitrogen, 13778-100) according to

the manufacturer's protocol. The detailed information of each siRNA or ASO used in this study is provided in Supplementary Table S2.

Western blotting

Protein extracts were prepared using RIPA buffer (50 mM/l Tris–HCl pH 7.4, 150 mM/L NaCl, 0.1% sodium dodecyl sulfate (SDS; w/v), 1% sodium deoxycholate (w/v), and 1% Triton X-100 (v/v)) and analyzed by western blotting as previously described (43–45). Briefly, protein samples were denatured at 100°C for 5 min in the presence of protein loading buffer (62.5 mM Tris–HCl pH 6.8, 10% glycerol (v/v), 0.01% bromophenol blue (w/v), 2.15% SDS (w/v), 1.55% dithiothreitol (w/v), and 5% 2-hydroxy-1-ethanethiol (v/v)), separated on 12% SDS-PAGE gels, and transferred to polyvinylidene fluoride (PVDF) membranes (BioRad, 1620177). Membranes were then processed following the standard ECL protocol (Thermo Fisher Scientific, EI9051). Blots were viewed using Bio-Rad ChemiDoc Imaging System and protein levels were quantified from at least three western blots using ImageJ. Antibodies used were anti-FLAG (Beyotime, AF519; 1:1000 dilution), anti-HDAC1 (Abcam, ab1767; 1:1000 dilution), anti-α-Tubulin (Beyotime, AF0001; 1:2000 dilution), and anti-Histone H3 (Abcam, ab1791; 1:1000 dilution).

Northern blotting

Northern blotting was performed as previously described (43,46). Briefly, the same amount of RNA was denatured at 65°C for 15 min in the presence of formaldehyde and Gel Loading Buffer II (Thermo Fisher Scientific, B8546G5), separated on 1.2% denaturing agarose gels, and transferred to hybond-N^+ membranes (GE healthcare, RPN303B). After UV crosslinking (254 nm, 120 mJ/cm^2), membranes were hybridized with DIG-labeled DNA probes (Sangon Biotech) at 42°C overnight followed by anti-DIG incubation for 2 h at room temperature using DIG Northern Starter Kit (Roche, 12039672910). Blots were viewed using Bio-Rad ChemiDoc Imaging System and RNA levels were quantified from at least three northern blots using ImageJ. The sequences of northern blotting probes are provided in Supplementary Table S3.

Estimating the RNase R resistance of *circSfl*

To confirm the resistance of *circSfl* to RNase R digestion, 15 μg of RNA from whole cells (the *circSfl* stable cell line) was treated with 10 units RNase R (Epicentre, RNR07250) for 20 min at 37°C, purified using RNAiso Plus (Takara, 9108), and subjected to northern blotting analyses.

Immunofluorescence staining

To visualize the subcellular localization of *circSfl*-derived Sfl protein (CdSfl) and *circPde8*-derived Pde8 protein (CdPde8), the *circSfl* and *circPde8* stable cell line were treated with 500 μM $CuSO_4$ for 12 h to induce protein expression. A total of 0.5×10^6 cells were seeded on a coverslip coated with concanavalin A (ConA; Solarbio, C8110) in a well of the 6-well plate for the final 2 hr. Coverslips (cell side up) were washed with 1 × PBS buffer (phosphate buffer saline pH 7.4: 137 mM NaCl, 2.7 mM KCl, 10 mM Na_2HPO_4 and 1.8 mM KH_2PO_4) twice and treated with fixative solution (75% methanol (v/v) and 25% glacial acetic acid (v/v)) for 10 min at room temperature. After washing the coverslips with TBST buffer (Tris-Buffered Saline Tween-20 pH 7.6: 0.242% Tris–HCl (w/v), 0.8% NaCl (w/v), and 0.05% Tween-20 (v/v)), cells were permeabilized with 0.1% Triton X-100 in TBST buffer at room temperature for 10 min. Coverslips were then treated with 5% bovine serum albumin (w/v; Beyotime, ST025) in TBST buffer to block non-specific binding of antibodies for 1 h followed by anti-FLAG (Beyotime, AF519) incubation at 4°C overnight. After washing the coverslips with TBST buffer for 3 times, cells were incubated with the Alexa Fluor 647 or 555 dye-labeled secondary antibody (Beyotime, A0473 and A0460) at room temperature for 2 h in the dark. 1 μg/ml DAPI (Beyotime, C1002) was used to stain nuclei for 10 min before imaging. A confocal laser scanning microscopy (Leica TCS, SP8) was used for imaging and ImageJ was used for quantification of nuclear and cytoplasmic fluorescence signals.

Estimating the half-life of *circSfl*

A total of 6.0×10^6 *circSfl* stable cells were treated with 500 μM $CuSO_4$ for 12 h to activate *circSfl* expression. Cells were washed with 1× PBS buffer twice and with the medium containing 500 μM bathocuproine disulphonate (BCS; Sigma, B1125) for 3 times. 50 μM BCS in fresh medium was then added for the indicated amounts of time (3, 6, 9, 12, 15, 18, 21 or 24 h) followed by RNA extraction and northern blotting analyses.

Estimating the half-life of CdSfl

A total of 6.0×10^6 *circSfl* stable cells were treated with 500 μM $CuSO_4$ for 12 h to activate CdSfl expression. Cells were washed with 1× PBS buffer twice and incubated with 100 μg/ml cycloheximide (CHX; Yeasen, 40325ES03) in fresh medium for the indicated amounts of time (1, 2, 3, 4, 5, 6, 7, 8 or 9 h) followed by protein extraction and western blotting analyses.

Estimating the sensitivity of CdSfl production to different translation inhibitors

A total of 1.2×10^7 *circSfl* stable cells were treated with the indicated inhibitor and 500 μM $CuSO_4$ simultaneously for 12 h followed by protein extraction and western blotting analyses. Translation inhibitors used in this experiment were anisomycin (ANS; 0.5 μg/ml; Apexbio, B6674), cycloheximide (CHX; 100 μg/ml; Yeasen, 40325ES03), homoharringtonine (HHT; 1 μg/ml; Apexbio, N1504), chloramphenicol (INN; 150 μg/ml; Biofroxx, 1289GR025), and rocaglamide-A (RocA; 0.3 μM; Apexbio, C5148).

Fluorescence *in situ* hybridization (FISH)

The FISH RNA probe against the back-splicing junction of *circSfl* was generated by *in vitro* transcription using

ScriptMAX® Thermo T7 Transcription Kit (TOYOBO, TSK-101), labeled with the Alexa Fluor 546 dye using ULYSIS® Nucleic Acid Labeling Kit (Thermo Fisher Scientific, U21652), and denatured at 95°C for 5 min before use. The sequence of the FISH probe is provided in Supplementary Table S4. To visualize the subcellular localization of *circSfl*, the *circSfl* stable cell line was treated with 500 μM $CuSO_4$ for 12 h to induce *circSfl* expression. A total of 0.5×10^6 cells were transferred onto a ConA-coated coverslip for the final 2 h, washed with ice-cold 1× PBS buffer twice, and treated with fixative solution (75% methanol (v/v) and 25% glacial acetic acid (v/v)) for 10 min at room temperature. Cells were then washed with 2× SSC Tween-20 buffer (300 mM NaCl, 30 mM sodium citrate, and 0.5% Tween-20 (v/v)), treated with 2 × SSC Triton X-100 buffer (300 mM NaCl, 30 mM sodium citrate, and 0.1% Triton X-100 (v/v)), denatured at 80°C for 10 min, and incubated with the FISH probe at 42°C in the presence of 20 ng/μl yeast RNA (Beyotime, R0038) overnight in the dark. 1 μg/ml DAPI (Beyotime, C1002) was used to stain nuclei for 10 min before imaging. A confocal laser scanning microscopy (Leica TCS, SP8) was used for imaging and Image J was used for quantification of nuclear and cytoplasmic fluorescence signals.

Cellular fractionation

To reveal the subcellular distribution of *circSfl* and CdSfl, cellular fractionation was performed as previously described (43,47). Briefly, the *circSfl* stable cell line was treated with 500 μM $CuSO_4$ for 12 h to induce *circSfl* and CdSfl expression. A total of 1.5×10^8 cells were washed with 1 ml of ice-cold 1× PBS buffer twice and resuspended in 1 ml of ice-cold lysis buffer I (10 mM Tris–HCl pH 8, 140 mM NaCl, 1.5 mM $MgCl_2$, 0.5% IGEPAL CA-630 (v/v), and 1 mM dithiothreitol) at 4°C followed by 100 rounds of pipetting. After spinning the cell lysate at 1000 × g for 3 min at 4°C, the cytoplasmic fraction was present in the supernatant of the centrifugate. The pellet was resuspended in 1.1 ml of ice-cold lysis buffer II (1 ml of lysis buffer I + 100 μl of detergent buffer [3.33% sodium deoxycholate (w/v) and 6.66% Tween-40 (v/v)]), slowly vortexed for 20 sec, and incubated on ice for 5 min. The mix was then spun at 1000 × g for 3 min at 4°C and washed with 1 ml of ice-cold lysis buffer I for 3 times. The final pellet was saved as the nuclear fraction. Efficient cellular fractionation was verified by examining the RNA levels of *rp49*, *U3* and *U6* and the protein levels of α-Tubulin and Histone H3 in each fraction.

Cross-linking immunoprecipitation (CLIP)

CLIP assays were performed as previously described (5,47). Briefly, cells were washed with ice-cold 1× PBS buffer twice, irradiated in a UV cross-linker (Lanyi, LYUV07-11) with 400 mJ/cm^2 at 254 nm on ice for 1 min, and incubated with RIPA buffer in the presence of RNase inhibitor (80 units/ml; Beyotime, R0102) and 1× Protease Inhibitor Cocktail (Beyotime, P1045) for 30 min on ice followed by 100 rounds of pipetting. After spinning the cell lysate at 12 000 × g for 5 min at 4°C, the supernatant of the centrifugate was saved as protein extracts and precleared with Protein A + G agarose beads (Beyotime, P2055) for 1 h at 4°C to prevent non-specific binding. Precleared protein extracts were incubated with the indicated antibodies or the negative IgG (as a control) for 4 h at 4 °C, and Protein A + G agarose beads (Beyotime, P2055) were then added to the mix for another 6 h at 4 °C. Beads were washed with RIPA buffer in the presence of RNase inhibitor (80 units/ml; Beyotime, R0102) for 4 times at 4°C and treated with 0.5 mg/ml proteinase K (Beyotime, ST535) for 30 min at 55°C to reverse cross-linking followed by RNA extraction and RT-qPCR analyses. Antibodies used in CLIP assays were anti-FLAG (Beyotime, AF519) and anti-V5 (Proteintech, 14440-1-AP).

To analyze the interaction between *circSfl* and the indicated eIFs, the notag *circSfl* stable cell line (*circSfl* from this cell line generates a non-tagged CdSfl) was transfected with the indicated plasmids of FLAG-tagged eIFs for 3 days. 500 μM $CuSO_4$ was added for the final 12 h to induce *circSfl* expression and cells were collected for CLIP assays.

To analyze the inhibitory effect of eIF3j on the binding of *circSfl* to eIF3 or Rps23, the notag *circSfl* stable cell line was depleted of eIF3j by dsRNA-mediated RNAi or overexpressed with eIF3j (V5-tagged) on day 1, transfected with the expression plasmid of FLAG-tagged eIF3a, eIF3b, or Rps23 on day 2, and collected for CLIP assays on day 4. 500 μM $CuSO_4$ was added for the final 12 h to induce *circSfl* expression.

To identify the functional domain of eIF3j which contributes to *circSfl* binding capacity, the *circSfl* stable cell line was transfected with the expression plasmid of the wild-type, N-terminus depleted, or C-terminus depleted eIF3j (V5-tagged) for 3 days. 500 μM $CuSO_4$ was added for the final 12 h to induce *circSfl* expression and cells were collected for CLIP assays.

To identify the UTR region where eIF3j recognizes, the notag *circSfl* stable cell line was transfected with the expression plasmid of FLAG-tagged eIF3j for 3 days. 500 μM $CuSO_4$ was added for the final 12 h to induce *circSfl* expression and cells were collected for iCLIP assays followed by RT-qPCR with 8 overlapping amplicons tiling through the *circSfl* UTR. iCLIP was performed as previously described with minor modifications (48).

To analyze the binding of the Δ101–200 *circSfl* mutant to the indicated eIF3 subunit (eIF3j, eIF3a or eIF3b), the Δ101–200 *circSfl* stable cell line (*circSfl* from this cell line is deleted of nucleotides 101–200 of the UTR) was transfected with the expression plasmid of the indicated eIF3 subunit (V5-tagged eIF3j, eIF3a, or eIF3b) for 3 days. 500 μM $CuSO_4$ was added for the final 12 hr to induce *circSfl* expression and cells were collected for CLIP assays. The binding of the wild-type *circSfl* and the Δ301–400 *circSfl* mutant to eIF3j, eIF3a, or eIF3b was also measured as a control.

To analyze the binding of *circSfl* to eIF3j in response to heat stress, the *circSfl* stable cell line was transfected with the expression plasmid of V5-tagged eIF3j for 3 days and maintained at 37°C for the final 4 h. 500 μM $CuSO_4$ was added for the final 12 h to induce *circSfl* expression and cells were collected for CLIP assays. The binding of *circSfl* to eIF3j under unstressed conditions was also measured as a control.

To analyze the binding of endogenous ribo-circRNAs to eIF3j, regular S2 cells were transfected with the expression

plasmid of FLAG-tagged eIF3j for 3 days and collected for CLIP assays.

To analyze the inhibitory effect of eIF3j on the binding of endogenous ribo-circRNAs to eIF3, regular S2 cells were depleted of eIF3j by dsRNA-mediated RNAi on day 1, transfected with the expression plasmid of FLAG-tagged eIF3a on day 2, and collected for CLIP assays on day 4.

The detailed information of plasmids used in these experiments is provided in the section 'plasmids and cloning' and Supplementary Plasmid Information.

RNA extraction and RT-qPCR

RNAs were extracted using RNAiso Plus (Takara, 9108) from whole cells, nuclear fractions, cytoplasmic fractions, or CLIP samples. Complementary DNAs (cDNAs) were generated by reverse-transcription using PrimeScript RT Master Mix (Takara, RR036A). QPCR assays were then conducted with the CFX connect real-time PCR system (Bio-Rad) using Hieff® qPCR SYBR Green Master Mix (YEASEN, 11201ES03) according to the manufacturer's protocol. For RNA extracts from whole cells, Ct values were normalized to the level of *rp49* mRNA. For RNA extracts from nuclear or cytoplasmic fractions, Ct values were calculated without any normalization (absolute Ct value). For RNA extracts from CLIP samples, signals (relative to input) were normalized to the negative IgG control. For semi-qPCR, the number of reaction cycles was set between 16 and 22 to avoid the saturation phase (49). The detailed information of qPCR primers is provided in Supplementary Table S5.

Estimating cellular sensitivity to stressed conditions

To examine the physiological function of *circSfl* or CdSfl in response to heat stress, S2 cells stably expressing the wild-type *circSfl* (WT) or the GCG mutant *circSfl* (GCG MUT) were cultured at 37°C for the indicated amounts of time (0, 1, 2 or 4 h). Cells were then stained with trypan blue (Biosharp, BS924) and counted using Bright-Line™ Hemacytometer (Sigma, Z359629).

Statistical analyses

Statistical significance for comparisons of means was assessed by Student's *t*-test ($^{**}P < 0.01$; $^{*}P < 0.05$). All data were generated from at least three independent biological replicates and are shown as means ± SEM in each figure legend.

RESULTS

Generation of a reporter vector for producing a translatable circRNA

For an efficient screening, we developed a translatable circRNA reporter vector by inserting the circularizing exon (including a FLAG sequence after the start codon) of the *Drosophila* gene *Sfl* between inverted intronic repeats of the previously described Hy_pMT laccase2 MCS exon vector (Figure 1A), which is able to efficiently express circRNAs under the control of a copper ion inducible promoter (p*MT*) (10). We chose *Sfl*-derived circRNA (*circSfl*) due to its known ability to generate a protein with a characterized physiological function in *Drosophila* (34). *CircSfl* uses the same start codon as its cognate mRNA and uses an in-frame stop codon downstream of the back-splicing junction (Figure 1A) (34). *CircSfl* expression in *Drosophila* S2 cells stably expressing the *circSfl* reporter was measured by northern blots and fluorescence *in situ* hybridization (FISH) with an antisense probe against the back-splicing junction (Figure 1B; Supplementary Figure S1A, B). Note that the vector-derived *circSfl* contains a multiple cloning site (MCS) sequence at the back-splicing junction such that the junction probe can specifically detect the vector-derived rather than endogenous *circSfl* (Figure 1A). We found that *circSfl* accumulated upon transcription induction over time and predominately localized in the cytoplasm (Figure 1B; Supplementary Figure S1A–C).

Further confirming that a true *circSfl* was produced, (i) the vector-derived transcript, but not ribosomal RNAs, was resistant to 3′-5′ exonuclease RNase R-mediated degradation (Figure 1C), (ii) the back-splicing junction-specific siRNA (circ siRNA) and ASO (circ ASO) significantly reduced the expression level of *circSfl* (Figure 1D, E), and (iii) Sanger sequencing of PCR products spanning across the junction site of *circSfl* revealed the ligated back-splicing exon (Supplementary Figure S1D, E). Moreover, transcription inhibition experiment, in which a 12 h transcription pulse was induced by copper sulfate and shut off by addition of the copper chelator bathocuproine disulphonate (BCS), demonstrated that *circSfl* had a long half-life of ∼15 h (Figure 1F, G). Finally, RT-qPCR revealed that *circSfl* expression of *circSfl* stable cells was ∼3000-fold higher than that of regular S2 cells (Supplementary Figure S1F). We thus concluded that the *circSfl* vector was efficiently back-spliced to produce a *bona fide* cytoplasmic circRNA.

Next, we detected a ∼25 kDa protein which corresponds to the expected protein size of *circSfl*-derived Sfl protein (CdSfl), and the level of the ∼25 kDa protein exhibited a similar trend to *circSfl* expression upon transcription induction (Figure 1B, H) or inhibition (Figure 1F, G, I, J), as verified by western blots with anti-FLAG. To further confirm the translation ability of *circSfl*, we verified that (i) the level of CdSfl drastically dropped to ∼10–20% when cells were individually transfected with the back-splicing junction-specific siRNA and ASO (Figure 1K, L), and that (ii) mutating the AUG start codon to a GCG codon or deleting the FLAG sequence did not affect *circSfl* expression, but resulted in CdSfl being no longer detected by western blots using anti-FLAG (Figure 1M, N). In addition, we found that CdSfl localized predominately in the cytoplasm (Supplementary Figure S2A-C) and had a half-life of ∼5 hr (Supplementary Figure S2D, E). Finally, translation inhibition experiment demonstrated that CdSfl was sensitive to the four examined translation inhibitors; note that it was not sensitive to the mitochondrial translation inhibitor chloramphenicol (INN) (Supplementary Figure S2F, G). These findings support that translatable circRNAs use factors similar to those in the canonical mRNA translation pathway.

Collectively, our results confirm identity of the ∼25 kDa protein and strongly support that the vector-derived *circSfl*

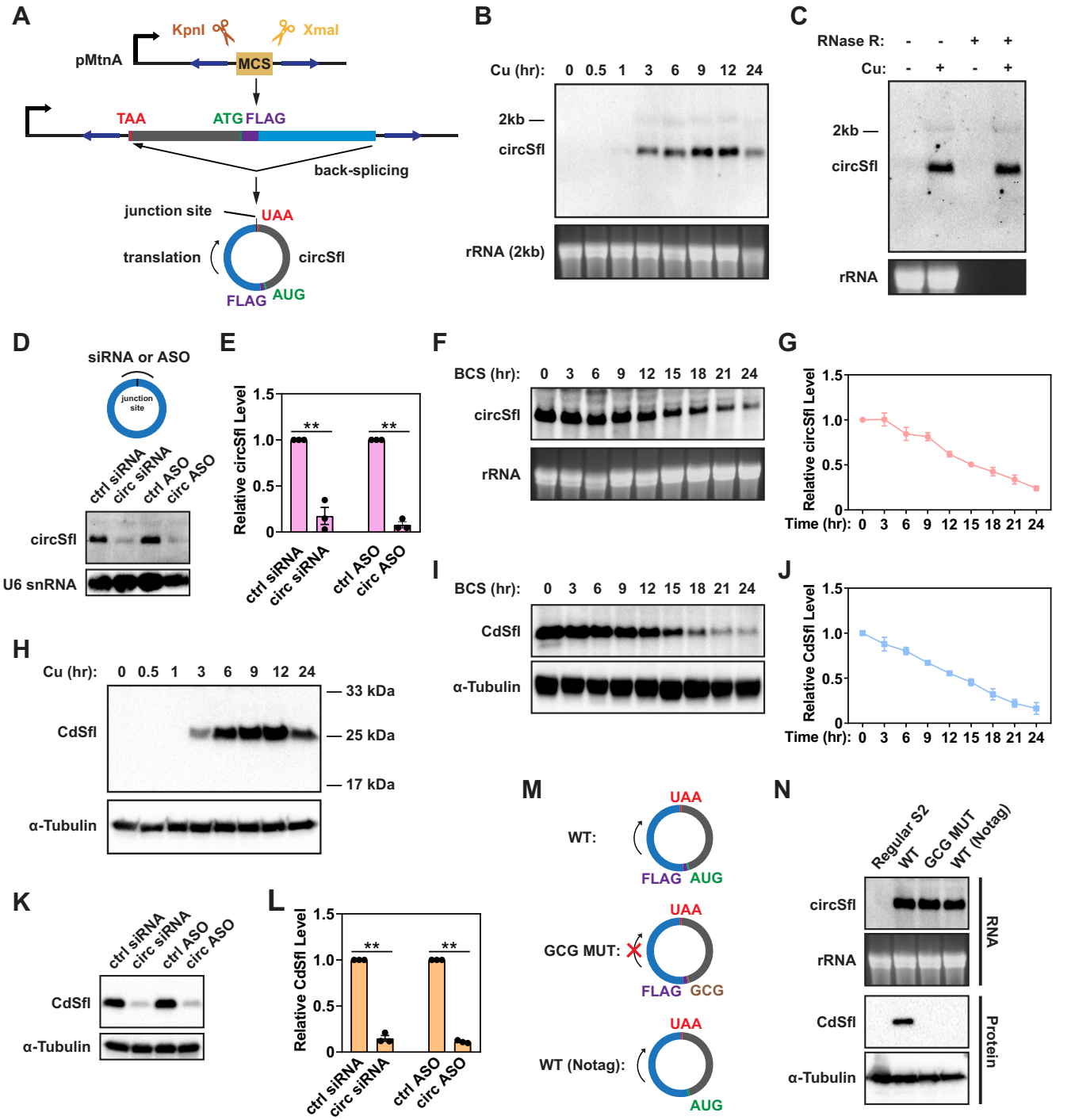

Figure 1. The *circSfl* reporter produces a readily detectable protein. (**A**) A schematic overview of the construction of the *circSfl* expression vector which is modified from the previously described Hy_pMT laccase2 MCS exon vector. The *circSfl* vector was used to generate a stable cell line using *Drosophila* S2 cells. (**B**) Northern blots with a probe against the *circSfl* back-splicing junction were performed to measure the expression of copper-activated *circSfl* in the stable line. (**C**) Northern blots of *circSfl* with RNAs digested with or without RNase R. RNA samples were extracted from the stable cell line treated with or without copper sulfate ($CuSO_4$). (**D, E**) Northern blots were performed to measure *circSfl* expression after the stable cell line had been individually transfected with the back-splicing junction-specific siRNA and ASO. *CircSfl* expression was quantified from three independent northern blots. $^{**}P < 0.01$; $^{*}P < 0.05$. (**F, G**) Northern blots of *circSfl* after a 12 h transcription pulse of *circSfl* had been induced by adding of copper into the stable line and shut off by sequestering copper with bathocuproine disulphonate (BCS). *CircSfl* expression was quantified from three independent northern blots. (**H**) Related to B, western blots were performed to measure CdSfl accumulation after the stable cell line had been induced with copper for the indicated amounts of time. (**I, J**) Related to F and G, western blots of CdSfl after the transcription of *circSfl* stopped. The CdSfl level was quantified from three independent western blots. (**K, L**) Related to D and E, western blots of CdSfl after *circSfl* had been knocked down. The CdSfl level was quantified from three independent western blots. $^{**}P < 0.01$; $^{*}P < 0.05$. (**M**) A schematic overview of the wild-type or mutant *circSfl*. (**N**) S2 cells stably expressing the wild-type or mutant *circSfl* were induced by copper for 12 hr. Northern and western blots were performed to measure the expression level of *circSfl* and CdSfl, respectively. All data were generated from at least three independent biological replicates and are shown as means ± SEM.

is efficiently translated into a readily detectable protein. We therefore envisioned that the *circSfl* stable cell line should enable an efficient screening and follow-up investigation for the underlying mechanism of circRNA translation.

RNAi screening reveals the inhibitory and promoting effect of different eIF3 subunits on the translational control of *circSfl*

In *Drosophila*, protein synthesis encompasses a series of initiation steps that are coordinated by 43 canonical *trans*-acting eIFs (50). To systematically evaluate the impact of eIFs on the translation initiation program of circRNAs, we took advantage of RNAi screening for all 43 eIFs in the *circSfl* stable cell line using dsRNAs. All dsRNAs were confirmed to efficiently knock down their targets (Supplementary Figure S3). Copper sulfate was added for the final 12 h to activate p*MT* and *circSfl* expression. Western blots and RT-qPCR were then performed to quantify the level of CdSfl and *circSfl*, respectively (Figure 2A). It is known that circRNAs are covalently-closed and thus lack a 7-methylguanylate (m^7G) cap structure which is recognized by the cap binding protein eIF4E and utilized by the canonical translation pathway (51–54). As expected, depletion of homologs of human eIF4E (e.g. eIF4E1 and eIF4E3) had a limited effect on *circSfl* translation (Figure 2B, C), confirming that circRNA translation initiation proceeds by a non-canonical mechanism.

To rule out the possibility that changes in *circSfl* translation were simply caused by altered *circSfl* biogenesis, we compared the level of CdSfl and *circSfl* in each knockdown sample and found that knockdown of some eIFs (e.g. eIF2α, eIF2γ, eIF1A, eIF4A and eIF4G1) resulted in a decreased expression of CdSfl and *circSfl* to a similar extent to each other (Figure 2B–D; Supplementary Screening Data), suggesting that these eIFs play a very limited role in the translation efficiency of *circSfl*. In support, the level of CdSfl was increased to a similar extent as that of *circSfl* when these eIFs were individually overexpressed (Figure 3A–D). Therefore, we concluded that a subset of eIFs, such as eIF2α, eIF2γ, eIF1A, eIF4A and eIF4G1, do not participate in the process of circRNA translation at least in the case of *circSfl*. We also noticed that several eIFs can function in both the translation and biogenesis of *circSfl*. A case in point is eIF2β, knockdown of which caused a ∼75% reduction in the CdSfl level and a ∼47% reduction in *circSfl* expression (Figure 2B–D; Supplementary Screening Data). The eIF2 complex is a very stable heterotrimer formed by eIF2α, eIF2β and eIF2γ in eukaryotic cells (51–54). The discrepancy of eIF2 components in our study could be explained by the assumption that the translation initiation of *circSfl* may proceed in an eIF2-independent manner. In fact, the final 80S initiation complex on certain linear mRNAs (e.g. c-Src mRNA) is still able to assemble without eIF2 (55–57). On the other hand, there are studies implying that eIF2β and eIF2γ may act in the absence of eIF2α under specific conditions (58). This raises another assumption that eIF2β might bring the initiator tRNA (Met-tRNAi) to the 40S ribosome without eIF2α and eIF2γ in the process of *circSfl* translation.

Notably, we identified that eIF3a, eIF3b, eIF3c and eIF3d1 were among the most potent positive regulators of *circSfl* translation, but did not affect *circSfl* expression (Figure 2B–D; Supplementary Screening Data). They were referred to positive eIF3 subunits herein. In eukaryotic cells, eIF3a and eIF3b function as the nucleation core of eIF3 for assembly of other eIF3 subunits into the octamer and the yeast-like core (YLC), respectively (37,59). The octameric head subunit eIF3c binds to eIF3a through its C-terminus and PCI (Proteasome-COP9 signalosome-eIF3) domain and was predicted to interact with ribosomal proteins near the mRNA exit channel (37,60–62). As a peripheral eIF3 subunit and a non-canonical cap-binding protein, eIF3d sits on the opposite site of the mRNA channel near the exit and directly interacts with the octameric right arm (41,63–65). To our surprise, the individual depletion of eIF3j, eIF3k, and eIF3l significantly elevated the extent of CdSfl production from the *circSfl* template (Figure 2B, C; Supplementary Screening Data). RT-qPCR investigating *circSfl* expression excluded the possibility that eIF3j, eIF3k, and eIF3l each inhibited *circSfl* biogenesis to limit its translation (Figure 2D; Supplementary Screening Data). We termed eIF3j, eIF3k and eIF3l as negative eIF3 subunits herein. As right leg subunits of the eIF3 octamer, eIF3k and eIF3l were found to be easily dissociated from the whole eIF3 complex and dispensable for eIF3 formation (59,65–67). eIF3j only loosely contacts with other eIF3 subunits and is usually considered as an eIF3-associated factor rather than a *bona fide* eIF3 subunit (37,68,69). Informed by the previous studies and the findings from our screening, we concluded that different eIF3 subunits can variously exert diametrically opposed functions regarding the translation of circRNA templates.

To confirm the phenotypes generated from our RNAi screening and rule out potential off-target effects of RNAi-directed knockdown, we took advantage of independent non-overlapping dsRNAs targeting the UTR of representative eIF3 subunits to repeat knockdown experiments and observed phenotypes that mirror our prior results (Figure 3E, F; Supplementary Figure S4). Moreover, we developed a series of expression vectors which only harbor the coding region of each examined eIF and are insensitive to UTR dsRNAs. Reexpression of these eIFs in cells treated with UTR dsRNAs significantly restored CdSfl production to levels similar to the 'β-gal' control sample (Figure 3E, F; Supplementary Figure S4). In addition, the involvement of eIF3 subunits in circRNA translation was recapitulated using a cell line stably expressing the *circSfl* vector modified from the previously described Hy_pMT dati Exons 1–3 vector (43,44,70), in which inverted intronic repeats of the *Drosophila* gene *dati* promote *circSfl* biogenesis (Supplementary Figure S5).

eIF3 interacts with *circSfl*

To understand the underlying mechanism for eIF3-mediated regulation, we applied cross-linking immunoprecipitation-reverse transcription-quantitative PCR (CLIP-RT-qPCR) to examine the recruitment of eIF3 subunits to *circSfl* (Figure 3G, H; Supplementary Figure S6A–D). We analyzed the CLIP-RT-qPCR results following the Fold Enrichment method, which is a signal-to-noise ratio comparing the amount of the target

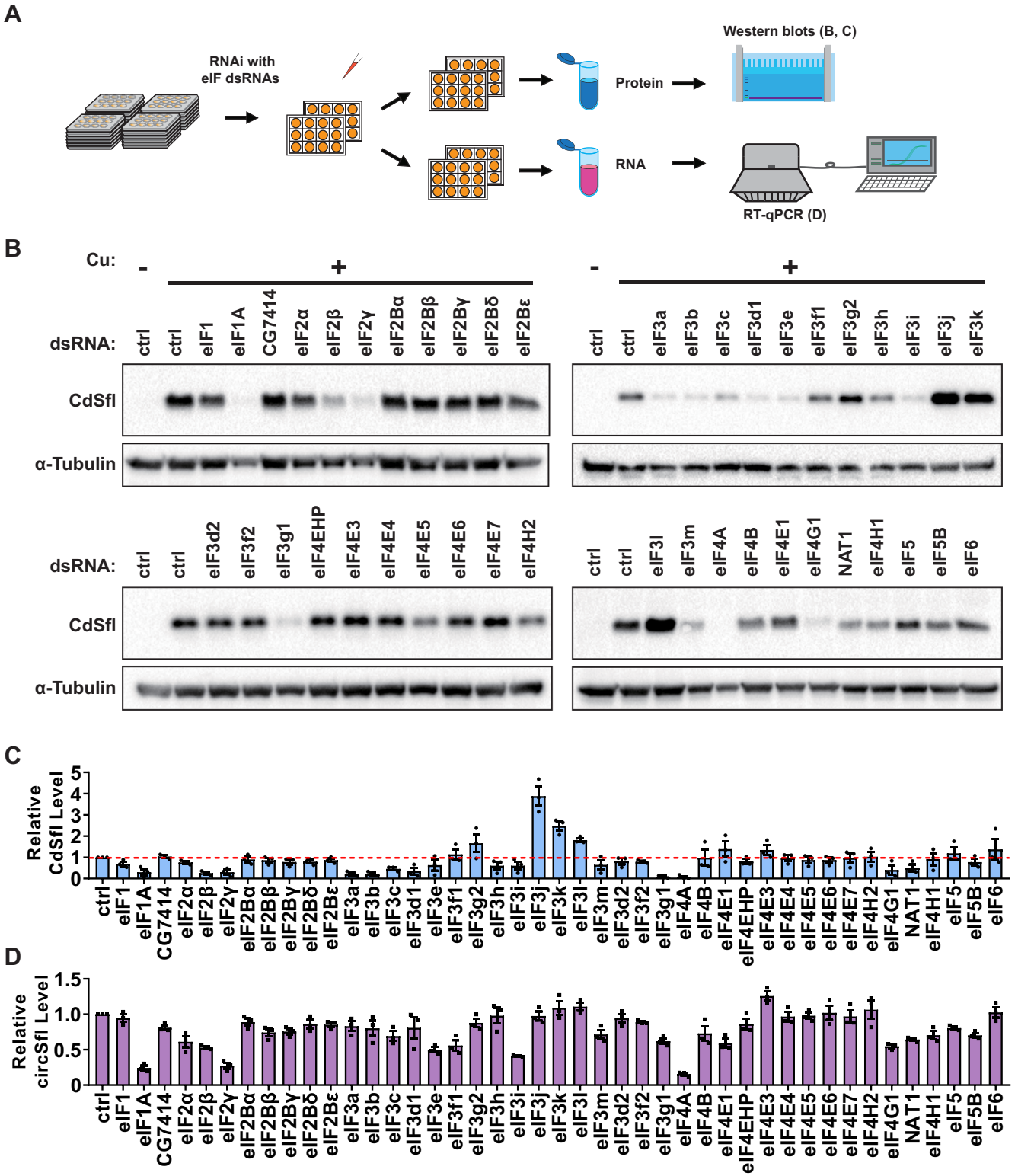

Figure 2. RNAi screening of eIFs that can regulate circRNA cap-independent translation. (**A**) A schematic overview of the RNAi screening strategy for identification of the impact of all 43 *Drosophila* eIFs on circRNA translation. The *circSfl* stable cell line was treated with each eIF dsRNA for 3 days and copper was added to induce *circSfl* expression for the final 12 h. β-gal dsRNA served as a negative control. (**B, C**) Western blots of CdSfl with protein extracts from the *circSfl* stable cell line treated with eIF dsRNAs. The CdSfl level was quantified from three independent western blots. (**D**) RT-qPCR was used to quantify *circSfl* expression using RNA extracts from the *circSfl* stable cell line treated with eIF dsRNAs. All data were generated from three independent biological replicates and are shown as means ± SEM.

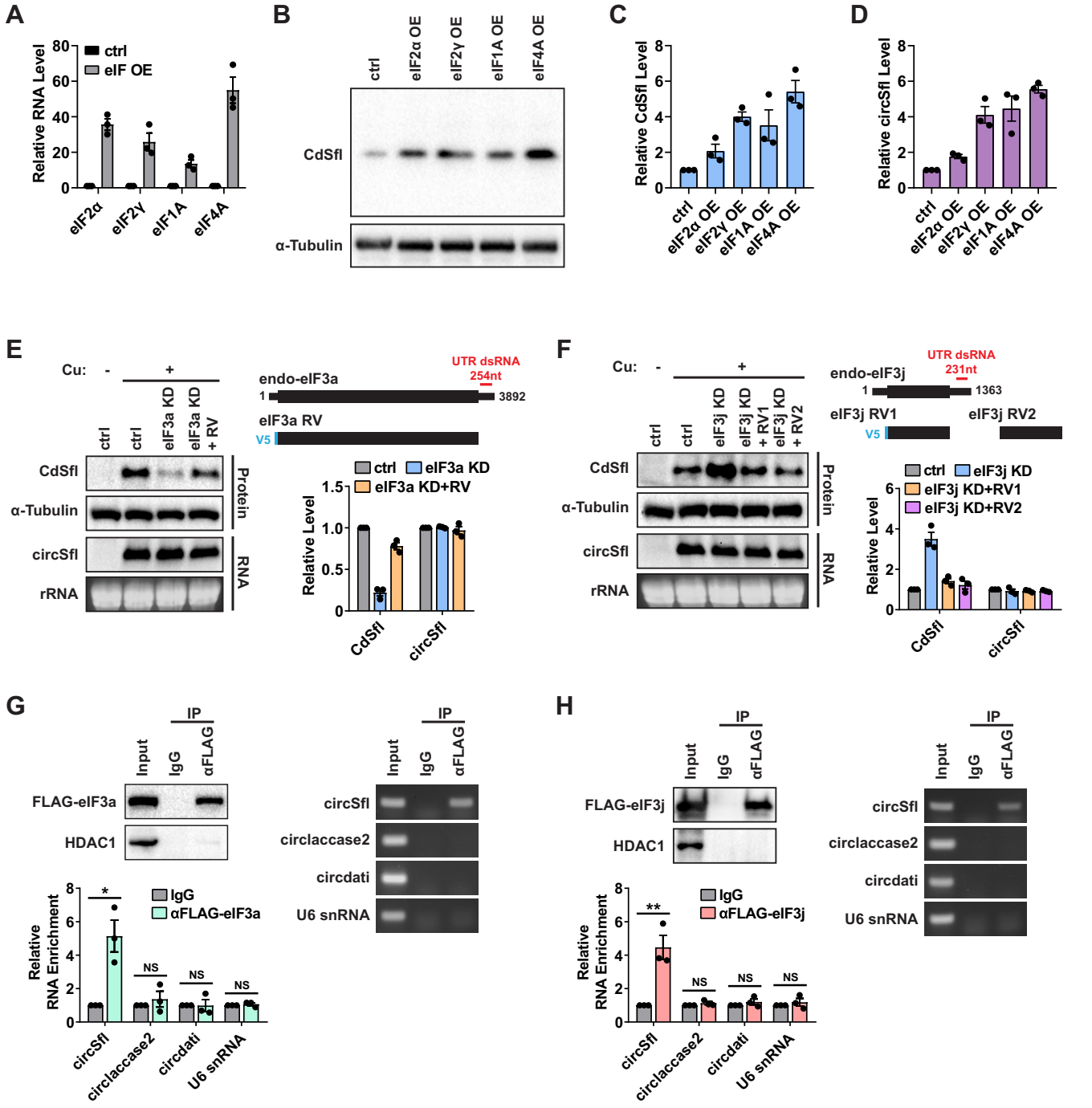

Figure 3. Identification of the conflicting functions of eIF3 subunits in the translational control of circRNAs. (**A**) RT-qPCR of the indicated eIF mRNAs after the *circSfl* stable cell line had been transfected with the indicated overexpression vectors. Empty vector served as a negative control. (**B, C**) Related to A, western blots of CdSfl examining the impact of the indicated eIFs on *circSfl* translation. The CdSfl level was quantified from three independent western blots. (**D**) Related to A, RT-qPCR of *circSfl* examining the impact of the indicated eIFs on *circSfl* biogenesis. (**E, F**) Rescue assays of the indicated eIF3 subunits using the *circSfl* stable cell line. UTR dsRNAs deplete endogenous but not vector-derived eIF3 subunits (V5-tagged). Western and northern blots were performed to detect CdSfl and *circSfl*, respectively. β-gal dsRNA served as a negative control. The level of CdSfl and *circSfl* were quantified from three independent blots. The gene locus and rescue vector (RV) of each eIF3 subunit with the location of the UTR dsRNA are also shown on the upper right panel. (**G, H**) CLIP assays of the indicated eIF3 subunits using the notag *circSfl* stable cell line (see Figure 1M). The expression vectors of FLAG-tagged eIF3 subunits were individually introduced into the notag *circSfl* stable cell line for 3 days. RT-qPCR and RT-semi-qPCR were performed with RNA extracts from CLIP samples to measure the binding of each eIF3 subunit to *circSfl*, *circlaccase2*, *circdati*, and *U6* snRNA. $^{**}P < 0.01$; $^{*}P < 0.05$. All data were generated from three independent biological replicates and are shown as means ± SEM.

sequence measured in the IP isolate (relative to input) to the amount measured in the negative control isolate. Unexpectedly, we observed that both positive and negative eIF3 subunits bound to *circSfl*, suggesting an interplay between positive and negative eIF3 subunits in the translational control of circRNAs. By contrast, control RNAs (without protein-coding ability, including *circlaccase2*, *circdati*, and *U6* snRNA) did not interact with the examined eIF3 subunits (Figure 3G, H, Supplementary Figure S6A–D). In addition, control eIFs, including eIF4E3 and eIF5, exhibited no significant binding capacity to *circSfl* (Supplementary Figure S6E, F). Considering that (i) depletion of eIF3j resulted in the largest increase in CdSfl production of all 43 eIFs screened (Figure 2; Supplementary Figure S5) and that (ii) eIF3j exhibited the strongest binding capacity to *circSfl* among the three negative eIFs (Figure 3H; Supplementary Figure S6C, D), we next focused on eIF3j-mediated circRNA translation repression and defined how the recruitment of different eIF3 subunits to translatable circRNAs leads to opposing translation phenotypes in the subsequent study.

eIF3j-mediated regulation is specific to the circular version of *Sfl* RNA

To explore whether eIF3j-mediated regulation is specific to *circSfl*, we constructed a vector which can exclusively produce a linear *Sfl* mRNA (Supplementary Figure S7A). Note that the sequence of this vector-derived linear *Sfl* mRNA is same to *circSfl*, and that the vector-derived linear *Sfl* mRNA can encode a protein whose amino acid sequence is same to CdSfl. The individual knockdown of eIF3a and eIF3b significantly reduced the Protein/RNA ratio (the relative linear *Sfl* encoded CdSfl level divided by the relative linear *Sfl* mRNA level), suggesting that the eIF3 complex is required for linear *Sfl* mRNA translation (Supplementary Figure S7B–E). In contrast to the results with *circSfl*, knockdown of eIF3j had no effect on the translation efficiency of the linear *Sfl* mRNA (Supplementary Figure S7B–E), ruling out that the linear *Sfl* mRNA is a subject of eIF3j-mediated regulation.

eIF3j inhibits the binding of eIF3 to *circSfl*

It is now known that eIF3a and eIF3b are the core subunits for the nucleation of the octamer and the YLC which are two interconnected modules of the eIF3 complex (Figure 4A) (37,59). eIF3 collapses without eIF3a and eIF3b (37,59). Codepletion experiments demonstrated that depletion of eIF3j did not increase CdSfl production in the absence of the nucleation core of eIF3 (Figure 4B–F), indicating that eIF3-mediated translation initiation is a prerequisite for the inhibitory role of eIF3j in the process of *circSfl* translation. In support of this, codepletion of eIF3c and eIF3j exhibited a similar phenotype (Supplementary Figure S8). In contrast to CdSfl, *circSfl* expression was only marginally affected upon codepletion of eIF3 subunits (Figure 4B–F; Supplementary Figure S8). Together, these results suggest a potential epistatic relationship in which the eIF3 complex binds to circRNAs and promotes their translation that may be subsequently monitored by eIF3j.

To explore whether eIF3j inhibits eIF3-mediated circRNA translation, CLIP-RT-qPCR was used to examine the impact of eIF3j on the recruitment of the nucleation core of eIF3 to *circSfl* (Figure 4G-K). Intriguingly, both eIF3a and eIF3b had a significantly increased ability to bind to *circSfl* when cells were depleted of eIF3j (Figure 4H, I), and overexpression of eIF3j resulted in the reduced binding of eIF3a and eIF3b to *circSfl* (Figure 4J, K). The binding of eIF3a and eIF3b to control RNAs (e.g. *circlaccase2* and the endogenous linear *Sfl* mRNA) was largely unaffected, thereby excluding the possibility of non-specific binding (Figure 4H–K). These results demonstrate that eIF3j represses circRNA translation by blocking the eIF3 complex from binding to translatable circRNAs.

eIF3j functions in *circSfl* translation through its C-terminus

We next aimed to identify the functional domain of eIF3j which contributes to the specialized translation repression, and a series of eIF3j mutant vectors were constructed (Figure 5A). Overexpression of the mutant eIF3j deleted of the C-terminus did not attenuate the extent of *circSfl* translation (Figures 5B, line 1 versus 6, C); however, mutants containing other deletions were still sufficient to inhibit CdSfl production, which is analogous to what was observed with the wild-type eIF3j (Figure 5B, line 1–5, C). Moreover, northern blots investigating *circSfl* expression excluded the possibility that these eIF3j mutants affected *circSfl* biogenesis/circularization (Figure 5B, C). These results indicate that the C-terminus of eIF3j is essential for eIF3j-mediated circRNA translation repression.

The C-terminus of eIF3j exhibits evolutionary conservation across eukaryotes (from *Drosophila* to human) (Supplementary Figure S9) and was predicted to bind to *circSfl* with a high discriminative power up to 68% (71). In line with the prediction, CLIP-RT-qPCR revealed that, compared with the wild-type eIF3j, the mutant with C-terminus deletion had a significantly reduced ability to bind to *circSfl* (Figure 5D). By contrast, no change was observed with the mutant with N-terminus deletion (Figure 5D). These results indicate that eIF3j recruitment to translatable circRNAs requires its C-terminus and is indispensable for its accurate function in translation repression. As a control, the binding of eIF3j to *circlaccase2*, *circdati*, *U6* snRNA, and the endogenous linear *Sfl* mRNA was not affected in the absence of the C-terminal region (Figure 5D), further confirming eIF3j-mediated translation repression is specific to *circSfl*. It is also worth noting that eIF3j can bind to the small ribosomal protein Rps23 occurring near the aminoacyl (A) site and mRNA entry channel of the 40S subunit, which subsequently blocks eIF3 loading to the A site and prevents mRNA recruitment (69,72). Notably, the C-terminus of eIF3j has been shown to be indispensable for the high affinity of eIF3j to the 40S subunit (69,72,73). Therefore, we next investigated the role of eIF3j in the interaction between *circSfl* and Rps23. As observed, neither knockdown nor overexpression of eIF3j interfered with the binding of Rps23 to *circSfl* (Figure 5E, F), somehow excluding the possibility that eIF3j blocks the recruitment of translatable circRNAs to ribosomes. Nonetheless, we cannot rule out that

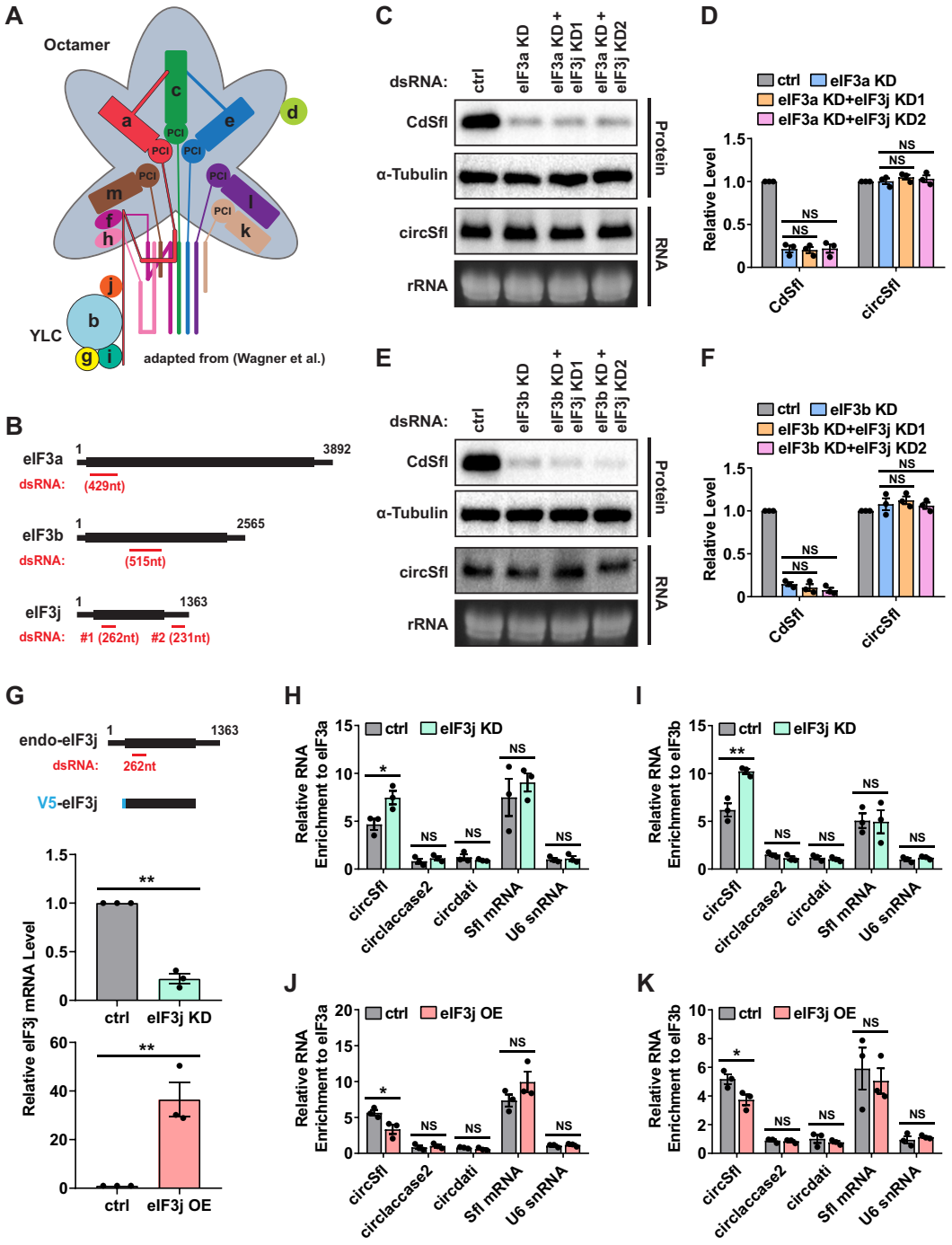

Figure 4. eIF3j inhibits circRNA translation by inducing the disassociation of the eIF3 complex from translatable circRNAs. (**A**) A schematic model of the eIF3 complex, adapted from (59). eIF3a and eIF3b serve as the nucleation core to bring other subunits together, while the eIF3-associated factor eIF3j only loosely interacts with other subunits. (**B**) The approximate locations of the indicated dsRNAs are shown at each gene locus for C–F. (**C, D**) Codepletion of eIF3a and eIF3j in the *circSfl* stable cell line. Western and northern blots were performed to detect CdSfl and *circSfl*, respectively. β-gal dsRNA served as a negative control. The level of CdSfl and *circSfl* were quantified from three independent blots. $^{**}P < 0.01$; $^{*}P < 0.05$. (**E, F**) Codepletion of eIF3b and eIF3j in the *circSfl* stable cell line. Western and northern blots were performed to detect CdSfl and *circSfl*, respectively. β-gal dsRNA served as a negative control. The level of CdSfl and *circSfl* were quantified from three independent blots. $^{**}P < 0.01$; $^{*}P < 0.05$. (**G**) The gene locus and overexpression vector of eIF3j with the approximate location of the indicated dsRNA are shown for H-K. RT-qPCR was performed to quantify the knockdown and overexpression efficiency of eIF3j. $^{**}P < 0.01$; $^{*}P < 0.05$. (**H, I**) CLIP assays of FLAG-tagged eIF3a (H) or eIF3b (I) using the notag *circSfl* stable cell line (see Figure 1M) depleted of eIF3j. β-gal dsRNA served as a negative control. RT-qPCR was performed with RNA extracts from CLIP samples to measure the binding of eIF3a (H) or eIF3b (I) to *circSfl*, *circlaccase2*, *circdati*, *U6* snRNA, and the endogenous linear *Sfl* mRNA. Data were normalized to the negative IgG sample. $^{**}P < 0.01$; $^{*}P < 0.05$. (**J, K**) CLIP assays of FLAG-tagged eIF3a (J) or eIF3b (K) using the notag *circSfl* stable cell line overexpressing V5-tagged eIF3j. Empty vector served as a negative control. RT-qPCR was performed with RNA extracts from CLIP samples to measure the binding of eIF3a (J) or eIF3b (K) to *circSfl*, *circlaccase2*, *circdati*, *U6* snRNA and the endogenous linear *Sfl* mRNA. Data were normalized to the negative IgG sample. $^{**}P < 0.01$; $^{*}P < 0.05$. All data were generated from three independent biological replicates and are shown as means ± SEM.

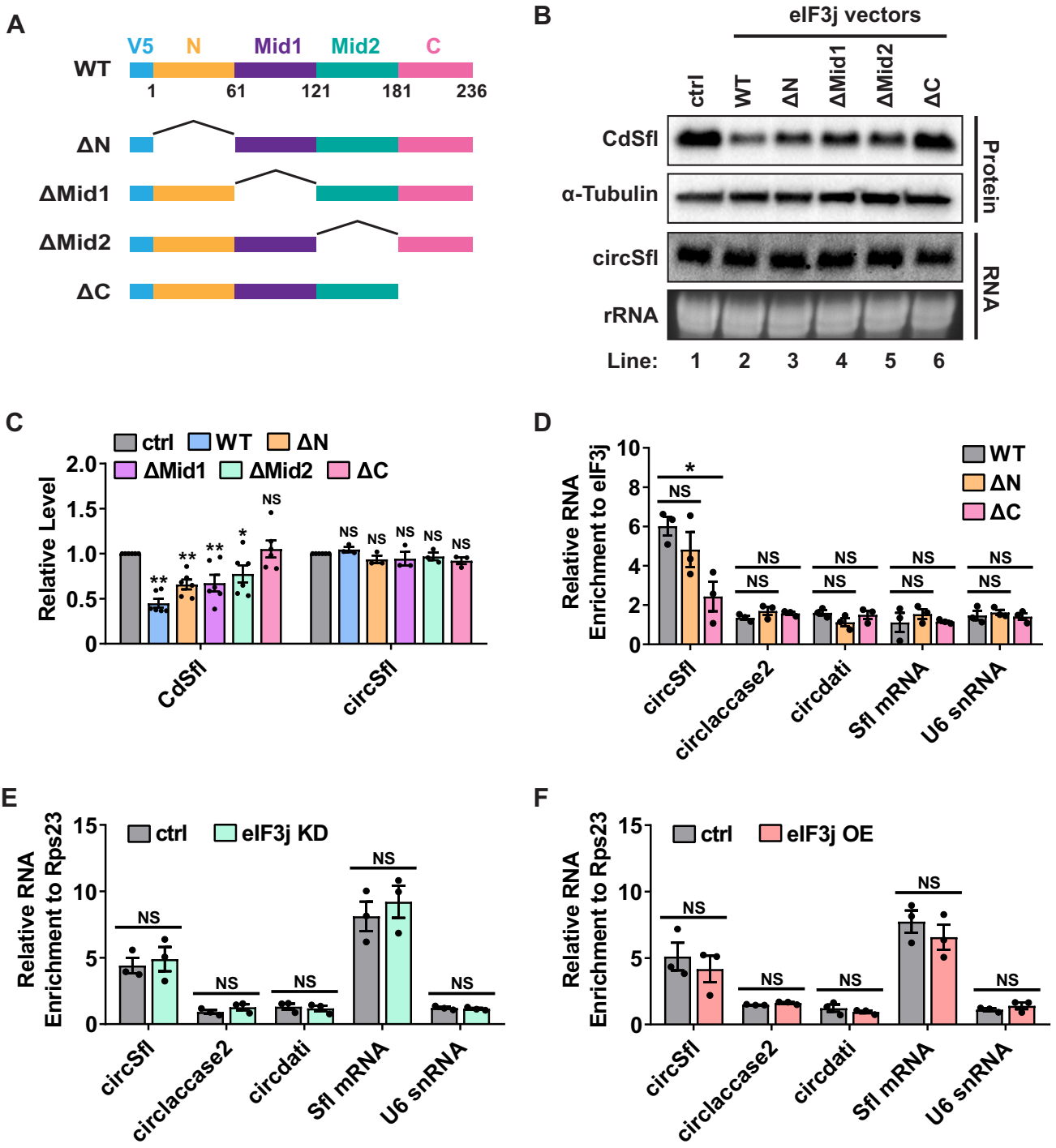

Figure 5. eIF3j-mediated circRNA translation repression is dependent of its C-terminus. (**A**) Schematics of eIF3j mutant vectors. (**B, C**) The individual overexpression of the wild-type and mutant eIF3j vectors in the *circSfl* stable cell line. Western and northern blots were performed to detect CdSfl and *circSfl*, respectively. Empty vector served as a negative control. The CdSfl level was quantified from six independent western blots and *circSfl* expression was quantified from three independent northern blots. $^{**}P < 0.01$; $^{*}P < 0.05$. (**D**) CLIP assays of the wild-type (WT), N-terminus depleted (ΔN), and C-terminus depleted (ΔC) eIF3j (V5-tagged) using the *circSfl* stable cell line. RT-qPCR was performed with RNA extracts from CLIP samples to measure the binding of the wild-type and mutant eIF3j to *circSfl*, *circlaccase2*, *circdati*, *U6* snRNA, and the endogenous linear *Sfl* mRNA. Data were normalized to the negative IgG sample. $^{**}P < 0.01$; $^{*}P < 0.05$. (**E**) CLIP assays of FLAG-tagged Rps23 using the notag *circSfl* stable cell line (see Figure 1M) depleted of eIF3j. β-gal dsRNA served as a negative control. RT-qPCR was performed with RNA extracts from CLIP samples to measure the binding of Rps23 to *circSfl*, *circlaccase2*, *circdati*, *U6* snRNA, and the endogenous linear *Sfl* mRNA. Data were normalized to the negative IgG sample. $^{**}P < 0.01$; $^{*}P < 0.05$. (**F**) CLIP assays of FLAG-tagged Rps23 using the notag *circSfl* stable cell line overexpressing V5-tagged eIF3j. Empty vector served as a negative control. RT-qPCR was performed with RNA extracts from CLIP samples to measure the binding of Rps23 to *circSfl*, *circlaccase2*, *circdati*, *U6* snRNA, and the endogenous linear *Sfl* mRNA. Data were normalized to the negative IgG sample. $^{**}P < 0.01$; $^{*}P < 0.05$. All data were generated from at least three independent biological replicates and are shown as means ± SEM.

eIF3j could block the access of eIF3 to *circSfl* by contacting Rps23 in the A site.

Taken together, we concluded that eIF3j makes specific interactions with translatable circRNAs, and these contacts, in turn, prevent the eIF3 complex from binding to circRNAs and initiating their translation.

Identification of the UTR region required for eIF3j-mediated *circSfl* translation repression

It has been previously reported that *cis*-acting RNA elements located in UTRs of protein-coding RNAs can provide additional layers of translational control to ensure proper protein expression (39,41,74,75). For example, the internal stem-loop structure embedded in the 5′ UTR of *c-Jun* mRNA blocks eIF4E-dependent translation to ensure eIF3d-specialized cap recognition (39,41). Given that *circSfl* harbors a 467 nt UTR, we thus tested whether an RNA regulon within the UTR of *circSfl* is functionally essential to eIF3j-mediated regulation. To this end, a series of *circSfl* mutant vectors containing truncated UTRs were generated and used for stable cell line construction (Figure 6A). Western and northern blots were performed to examine the level of CdSfl and *circSfl*, respectively. Of five *circSfl* UTR mutants, four (Δ1–100, Δ201–300, Δ301–400 and Δ401–467) yielded a reduction in CdSfl production, suggesting that these UTR regions promote circRNA translation. Particularly, the translation of *circSfl* was barely detectable when the *circSfl* UTR was individually deleted of nucleotides 1–100, 201–300 and 401–467 (Figure 6B, C). Note that *circSfl* expression also dropped to ∼43% upon deletion of nucleotides 201–300, indicating that the decreased CdSfl production of the Δ201–300 mutant was attributed to a combination of the reduced biogenesis and translation of *circSfl* (Figure 6B, C).

By contrast, the CdSfl level had a ∼69% increase when the *circSfl* UTR was deleted of nucleotides 101–200, despite a ∼26% reduction in *circSfl* expression. This indicates that nucleotides 101–200 negatively regulate *circSfl* translation, which is distinct from the results from other four UTR regions (Figure 6B, C). Next, we individually knocked down eIF3a and eIF3b using the Δ101–200 *circSfl* stable cell line and observed that, although there was no change in *circSfl* expression, *circSfl* failed to produce CdSfl in the absence of the nucleation core of eIF3 (Figure 6D–F). This suggests that the translation of the mutant *circSfl* lacking nucleotides 101–200 of the UTR is still in an eIF3-dependent manner, which is consistent with the result from the wild-type *circSfl*. It is known that GC-rich RNA elements in UTRs have the potential to form a stable secondary structure to block ribosome scanning (76). In the case of *circSfl*, the GC content of nucleotides 101–200 of the UTR is only 40% (Figure 6G). It is thus unlikely that this UTR region intrinsically impedes circRNA translation initiation, which is supported by the RNAfold structure prediction (Figure 6G) (77,78). Instead, this UTR region may rely on other *trans*-acting factors, such as eIF3j, to exert its inhibitory role.

Therefore, we tested the functional relevance of nucleotides 101–200 to eIF3j. To identify the UTR region where eIF3j recognizes, iCLIP-RT-qPCR experiments were performed with 8 overlapping amplicons tiling through the UTR of *circSfl*. We found that eIF3j exhibited a higher binding capacity to nucleotides 101–200 compared to other UTR regions (Figure 6H). In addition, neither depletion nor overexpression of eIF3j affected CdSfl production of the Δ101–200 mutant (Figure 6I-K), in contrast to the phenotypes obtained from the wild-type *circSfl* (Figure 6L, M) and the Δ301–400 mutant (Supplementary Figure S10A, B). Note that we also examined the effect of eIF3j knockdown on *circSfl* translation using the Δ1–100 and Δ401–467 *circSfl* stable cell line. No change was observed with the CdSfl level, indicating that Δ1–100 and Δ401–467 are simply dead mutants (Supplementary Figure S10C–F). These results thus support that the fate of undergoing eIF3j-mediated translational regulation is encrypted in the context of nucleotides 101–200 of the *circSfl* UTR. To further gain a mechanistic insight into how this *cis*-acting RNA regulon coordinates eIF3j, CLIP-RT-qPCR was used to examine eIF3j recruitment to the Δ101–200 mutant. Compared with the wild-type *circSfl*, this mutant almost completely lost the ability to interact with eIF3j (Figure 6N, O). Correspondingly, the binding of the nucleation core of eIF3 to the Δ101–200 mutant exhibited a significant increase (Figure 6N, P, Q). As a control, the binding of the Δ301–400 mutant to eIF3a, eIF3b, and eIF3j was not altered (Figure 6N–Q). Taken together, these findings demonstrate that nucleotides 101–200 of the *circSfl* UTR facilitate the binding of eIF3j to *circSfl*, and, in turn, ensure the inhibitory effect of eIF3j on the eIF3 complex.

eIF3j-mediated translational regulation in response to stressed conditions

The expression of circRNAs is perturbed in response to various stresses and a great many circRNAs serve as regulatory factors under different physiological or pathological conditions to maintain cellular homeostasis (16–20). Notably, emerging studies have demonstrated that some circRNAs exert functions through their encoded proteins instead of themselves (31–33). However, the physiological relevance of eIF3j-mediated circRNA translation program remains an unknown question. To fill this gap, S2 cells stably expressing the wild-type *circSfl* (WT) or the GCG mutant *circSfl* (GCG MUT) were used for the subsequent study (Figure 1M, N). Considering that the endogenous *circSfl* is weakly expressed in the regular S2 cell line (Supplementary Figure S1F) (46,79), these *circSfl* stable cell lines served as ideal models of *circSfl* highly expressed cells or tissues (e.g. neuronal cells (34)) with no or marginal influence from the endogenous *circSfl*. In addition, it was easy to distinguish the physiological role of CdSfl from that of *circSfl*, since GCG MUT cells only generate the mutant *circSfl* without translation ability (Figure 1M, N).

Given that *circSfl* was found to be a type of insulin-sensitive circRNAs (34) and that heat shock response is involved in the regulation of insulin sensitivity (80), we thus investigated the potential physiological role of *circSfl* and CdSfl in response to heat stress. After heat shock treatment, the number of stressed cells was counted. Compared with regular S2 cells and GCG MUT cells, WT cells exhibited a significant resistance to heat stress (Figure 7A). In addition, neither *circSfl* nor CdSfl affected cell proliferation un-

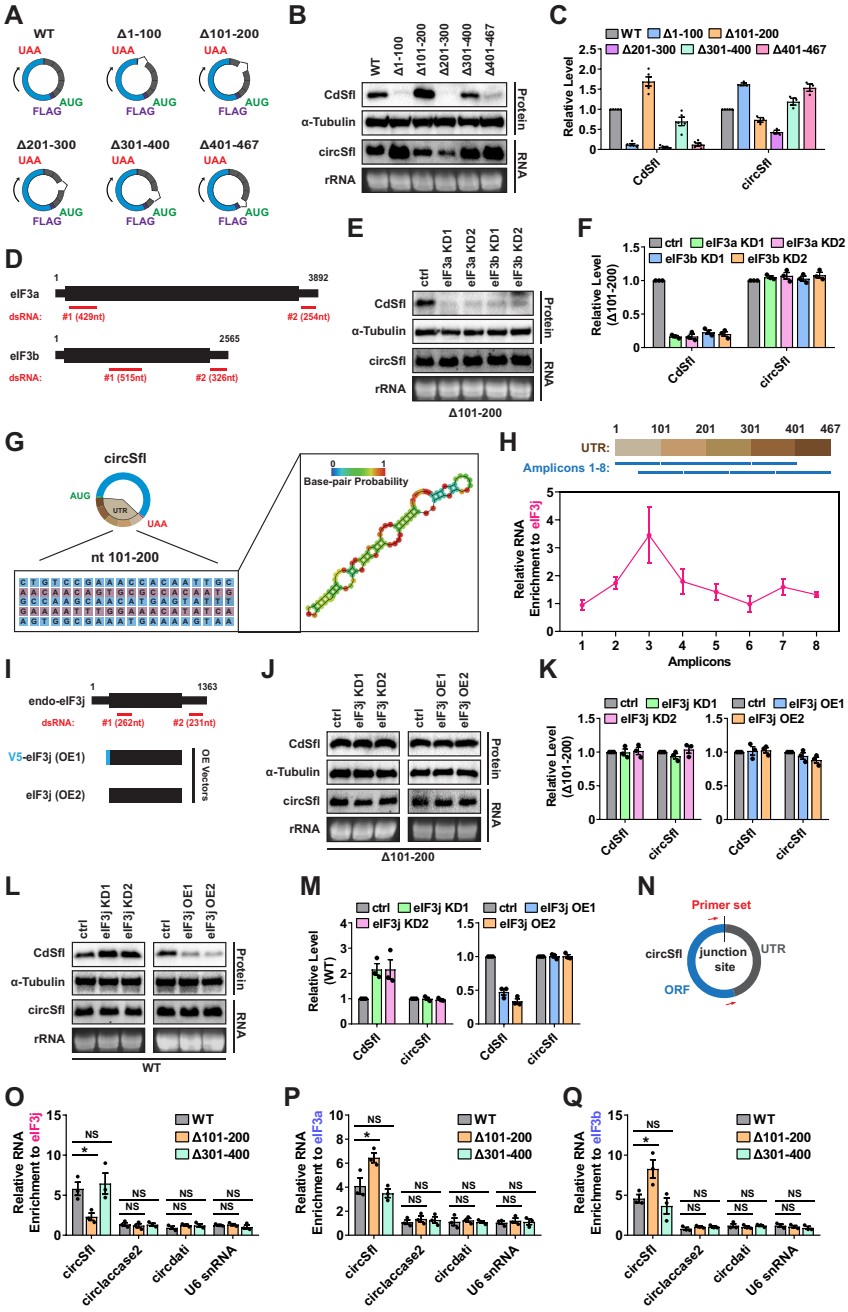

Figure 6. Identification of the UTR region required for the inhibitory effect of eIF3j on the eIF3 complex. (**A**) Schematics of *circSfl* mutants containing truncated UTRs (Δ1–100, Δ101–200, Δ201–300, Δ301–400 and Δ401–467). (**B, C**) Western and northern blots were performed to detect CdSfl and *circSfl* in S2 cells stably expressing these *circSfl* mutants. The CdSfl level was quantified from five independent western blots and *circSfl* expression was quantified from three independent northern blots. (**D**) The approximate locations of the indicated dsRNAs are shown at each gene locus for E and F. (**E, F**) Western and northern blots were performed to detect CdSfl and *circSfl* in the Δ101–200 *circSfl* stable cell line depleted of eIF3a or eIF3b. β-gal dsRNA served as a negative control. The level of CdSfl and *circSfl* were quantified from three independent blots. (**G**) The nucleotide sequence and a possible secondary structure of nucleotides 101–200 of the *circSfl* UTR. (**H**) iCLIP assays of FLAG-tagged eIF3j using the notag *circSfl* stable cell line (see Figure 1M). 8 overlapping amplicons were used to tile through the UTR of *circSfl*. Data were normalized to the negative IgG sample. (**I**) The gene locus and overexpression vectors of eIF3j with the approximate locations of the indicated dsRNAs are shown for J–M. (**J, K**) Western and northern blots were performed to detect CdSfl and *circSfl* in the Δ101–200 *circSfl* stable cell line depleted of eIF3j (J, left panel) or overexpressing eIF3j (J, right panel). β-gal dsRNA and empty vector served as a negative control in these depletion and overexpression experiments, respectively. The level of CdSfl and *circSfl* were quantified from three independent blots. (**L, M**) Western and northern blots were performed to detect CdSfl and *circSfl* in the *circSfl* stable cell line depleted of eIF3j (L, left panel) or overexpressing eIF3j (L, right panel). β-gal dsRNA and empty vector served as a negative control in these depletion and overexpression experiments, respectively. The level of CdSfl and *circSfl* were quantified from three independent blots. (**N**) The primer set spanning across the junction site and the UTR of *circSfl* was used for O–Q. (**O–Q**) CLIP assays of V5-tagged eIF3j (O), eIF3a (P), and eIF3b (Q) using the *circSfl* stable cell line and the *circSfl* mutant stable cell line (Δ101–200 and Δ301–400). RT-qPCR was performed with RNA extracts from CLIP samples to measure the binding of the indicated eIF3 subunits to the wild-type and mutant *circSfl*. Data were normalized to the negative IgG sample. $^{**}P < 0.01$; $^{*}P < 0.05$. All data were generated from at least three independent biological replicates and are shown as means ± SEM.

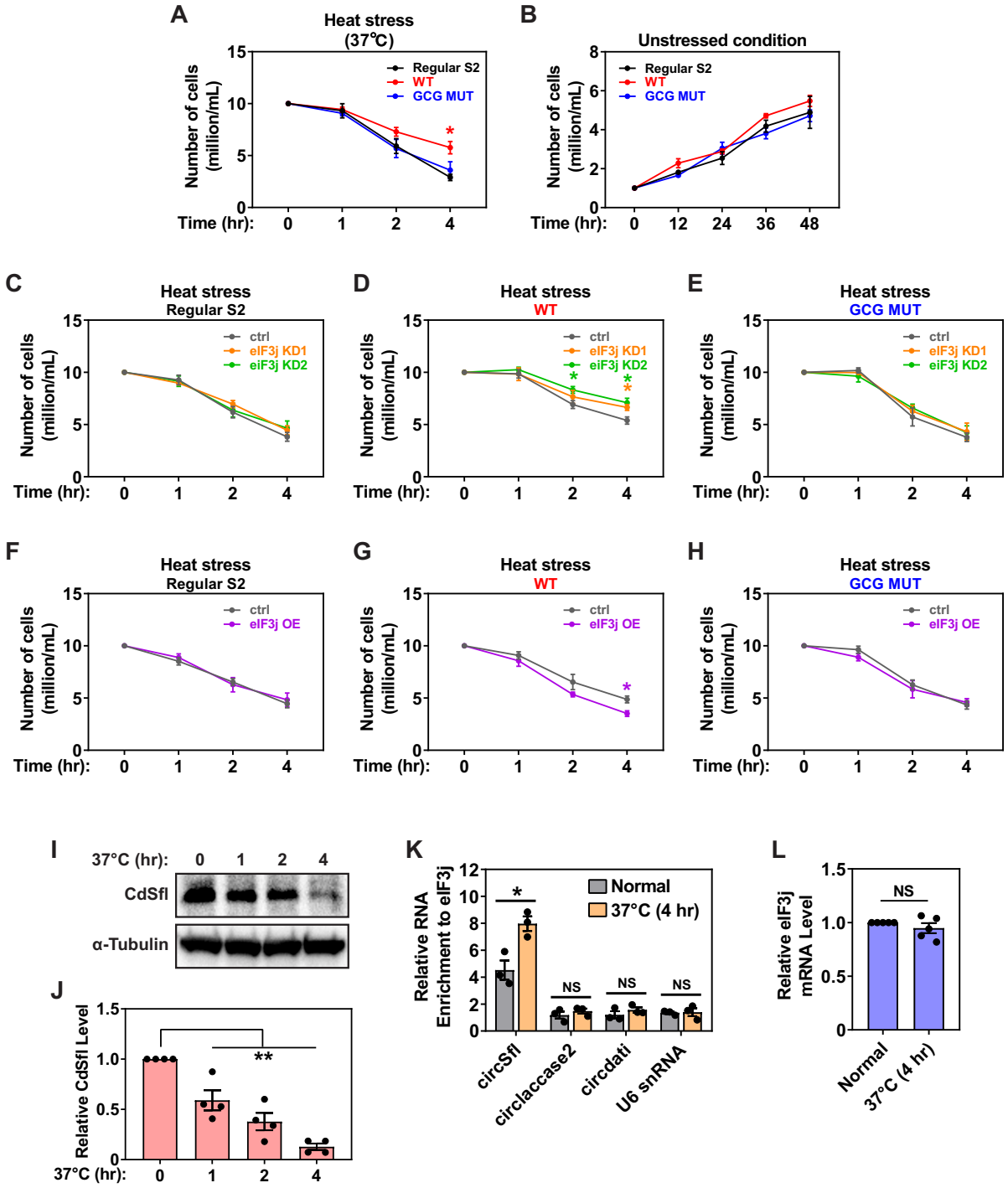

Figure 7. The physiological relevance of eIF3j-mediated translation repression in cellular response to stressed conditions. (**A**) Examination of cellular resistance to heat shock. S2 cells stably expressing the wild-type *circSfl* (WT) or the GCG mutant *circSfl* (GCG MUT; see Figure 1M) were cultured at 37°C for the indicated amounts of time and the number of stressed cells was counted. The resistance of regular S2 cells served as a negative control. $^{**}P < 0.01$; $^{*}P < 0.05$. (**B**) Examination of cell proliferation of the indicated cell line under unstressed conditions. The number of cells was counted at different time points. $^{**}P < 0.01$; $^{*}P < 0.05$. (**C–E**) Examination of cellular resistance of the indicated cell line to heat shock after cells had been depleted of eIF3j. The number of heat-shocked cells was counted at different time points. β-gal dsRNA served as a negative control. $^{**}P < 0.01$; $^{*}P < 0.05$. (**F–H**) Examination of cellular resistance of the indicated cell line to heat shock after cells had overexpressed V5-tagged eIF3j. The number of heat-shocked cells was counted at different time points. Empty vector served as a negative control. $^{**}P < 0.01$; $^{*}P < 0.05$. (**I, J**) Western blots of CdSfl with protein extracts from the heat-shocked *circSfl* stable cell line. The CdSfl level was quantified from four independent western blots. $^{**}P < 0.01$; $^{*}P < 0.05$. (**K**) CLIP assays of V5-tagged eIF3j using the unstressed and heat-shocked *circSfl* stable cell line. RT-qPCR was performed with RNA extracts from CLIP samples to measure the binding of eIF3j to *circSfl*, *circlaccase2*, *circdati*, and *U6* snRNA. Data were normalized to the negative IgG sample. $^{**}P < 0.01$; $^{*}P < 0.05$. (**L**) RT-qPCR quantification of the endogenous *eIF3j* mRNA in the unstressed and heat-shocked *circSfl* stable cell line. $^{**}P < 0.01$; $^{*}P < 0.05$. All data were generated from at least three independent biological replicates and are shown as means ± SEM.

der unstressed conditions (Figure 7B). These findings support that *circSfl* only functions through its encoded protein CdSfl during heat stress.

Based on the above observation, we next asked whether eIF3j affects heat resistance through modulating *circSfl* translation. Depletion of eIF3j significantly increased the heat resistance of WT cells but not regular S2 cells or GCG MUT cells (Figure 7C–E). Moreover, overexpression of eIF3j significantly reduced the heat resistance, which is also specific to WT cells (Figure 7F-H). These results imply that eIF3j physiologically reduces heat resistance through down-regulation of CdSfl production. In support, the CdSfl level exhibited a remarkable decrease during heat stress over time (Figure 7I, J). Particularly, CdSfl was almost completely eliminated after 4 hr heat shock (Figure 7I, J). Mechanistically, eIF3j recruitment to *circSfl* was significantly elevated in response to heat shock (Figure 7K), despite no change in *eIF3j* expression (Figure 7L). Taken together, these findings indicate that eIF3j is able to physiologically regulate heat resistance through modulating circRNA translation, thereby ensuring clean of damaged cells.

eIF3j regulates translation of a subset of circRNAs

To explore whether eIF3j-mediated regulation represents a widespread mechanism for circRNA translation, we examined the binding of eIF3j to 15 previously annotated endogenous ribo-circRNAs, which were identified by ribosome footprinting from S2 cells (28). As observed, four were found to significantly interact with eIF3j (Figure 8A). Among these four eIF3j-associated ribo-circRNAs, three (e.g. *circPde8*) exhibited a significantly increased binding capacity to the nucleation core of eIF3 upon eIF3j knockdown (Figure 8B), which is similar to what was observed with *circSfl* (Figure 4H, I). To further validate the role of eIF3j in translation repression of other circRNAs, we chose *circPde8* for subsequent experiments and constructed a cell line stably expressing *circPde8* (Figure 8C). The *circPde8* stable cell line was confirmed to successfully generate a cytoplasmic protein (Figure 8D, E), which was referred to *circPde8*-derived Pde8 (CdPde8) herein. Knockdown of eIF3a and eIF3b reduced the translation efficiency of *circPde8*, while knockdown of eIF3j elevated the level of CdPde8 (Figure 8F, G). The RNA level of *circPde8* was almost not affected in above knockdown experiments (Figure 8H), excluding the possibility of altered *circPde8* biogenesis. Taken together, these results support that eIF3j inhibits translation of at least a subset of circRNAs in *Drosophila* S2 cells.

DISCUSSION

eIFs in circRNA translation

Due to the sequence homology between circRNAs and their linear counterparts, circRNA-derived proteins usually share the same amino acid sequence (or even the same start codon) with their cognate full-length proteins (34,81), implying that the functions of these novel truncated proteins are somehow auxiliary to their full-length versions. Indeed, the *circSMO*-derived protein SMO193aa, identical to amino acids 230–421 of the full-length SMO, can promote SMO-mediated Hedgehog signaling activation and tumorigenicity in glioblastoma patients (81). However, some circRNA-derived proteins have distinct subcellular localizations and biological functions compared to their full-length versions (82). A case in point is *circARHGAP35* whose encoded protein promotes cancer progression by forming a complex with the transcription factor TFII-I in the nucleus, whereas the full-length ARHGAP35 inhibits tumor growth by switching off RhoA activity in the cytoplasm (82). These studies indicate that (i) circRNA-derived proteins are not a simple supply to the full-length cognates, (ii) the accurate control of circRNA translation is fundamental to pattern biological processes, and (iii) cells require a mechanism to specifically coordinate the translation of these novel proteins. In this study, we evaluated the impact of all *Drosophila* eIFs on circRNA translation and the focused investigation regarding *circSfl* proposes the molecular mechanism of eIF3j-mediated translational control: eIF3j interacts with translatable circRNAs and inhibits translation by preventing the eIF3 complex from binding to circRNA templates (or displacing eIF3 from templates) (Figure 9), providing a pathway that assists the general translational machinery to specifically recognize circRNA templates. The inhibitory activity of eIF3j requires its C-terminus and relies on an RNA regulon located in the circRNA UTR. Moreover, we revealed that the binding of eIF3j to circRNAs varies in response to stressed conditions, thereby influencing the translation ability of stress-responsive circRNAs and, in turn, cellular physiology. In summary, our study provides a significant insight into the field of cap-independent transcript-specific translation.

It is important to emphasize that eIF3j was also shown to directly interact with Rps23 in the ribosomal decoding center (69,72) and the C-terminus of eIF3j is required for its binding to the 40S ribosomal subunit (69,73), reminiscent of the phenotype that the C-terminus of eIF3j facilitates its recruitment to translatable circRNAs (Figure 5A-D). In this regard, we observed that eIF3j was not involved in the association between Rps23 and circRNAs (Figure 5E, F). Therefore, it is not likely that eIF3j prevents the recruitment of translatable circRNAs to ribosomes. But this hypothesis needs to be further validated. Moreover, the binding capacity of eIF3j to the 40S subunit decreases in the presence of linear mRNAs (83,84). We thus speculate a possible role of eIF3j in discrimination of circular and linear translation templates. On the other hand, an interplay between eIF3j and eIF1A has also been revealed (69,72,85,86). They can bind anticooperatively to the 40S subunit surface (69,86) or closely cooperate to orchestrate the process of AUG recognition (72). However, no robust impact of eIF1A on *circSfl* translation was observed in our screening. eIF1A seems to regulate *circSfl* biogenesis to affect the expression level of CdSfl (Figure 2B-D). Taken together, the previous findings as well as our study strongly support that eIF3j represents a regulatory/accessory factor for eIF3 and is not a *bona fide* eIF3 subunit.

In addition to eIF3j, two tightly interacting octameric partners eIF3k and eIF3l were also found to robustly inhibit *circSfl* translation in our screening (Figure 2B-D), suggesting that they can exert a function different from the canonical role of eIF3. In support, only eIF3k and eIF3l are

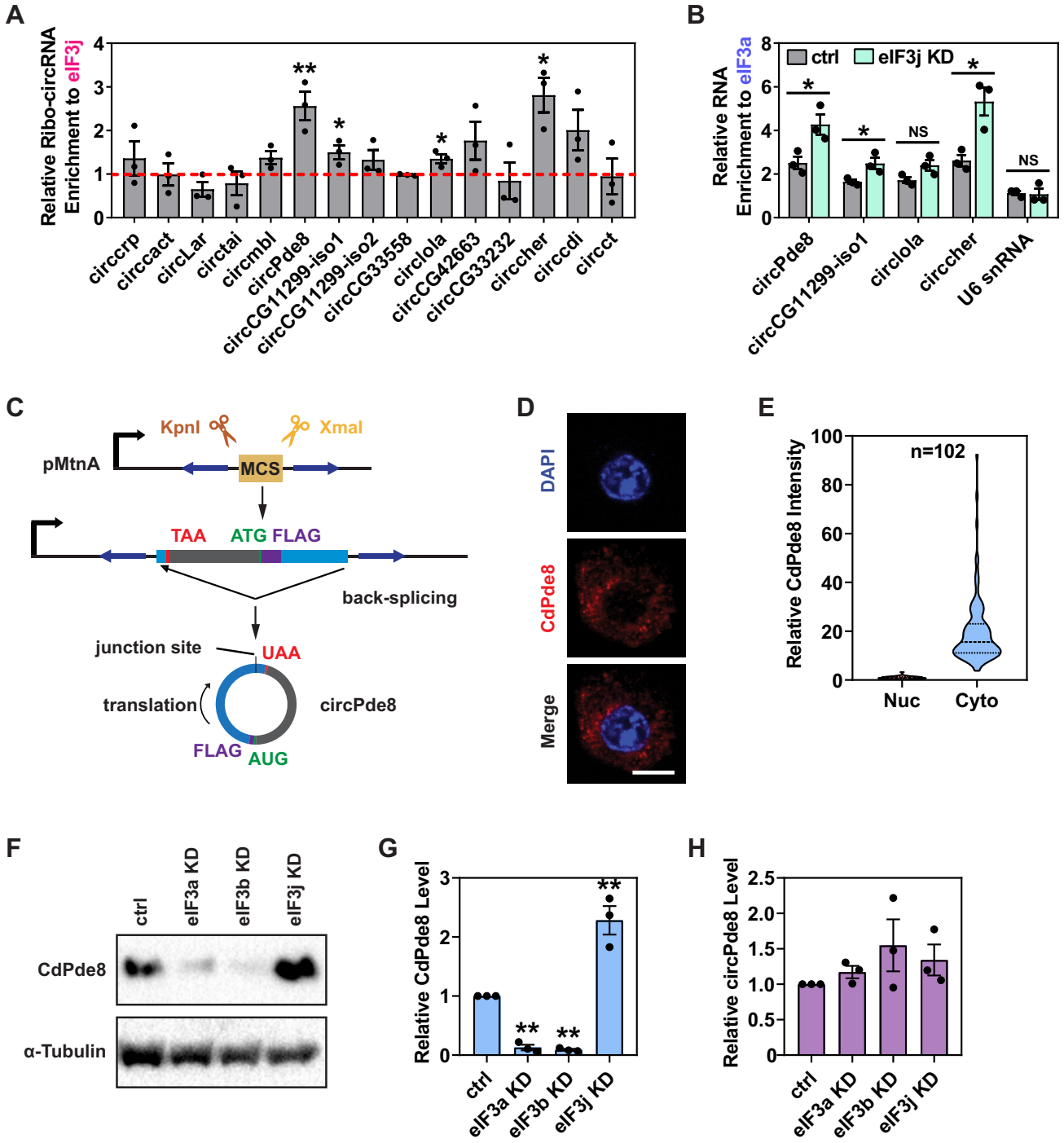

Figure 8. eIF3j regulates translation of additional circRNAs. (**A**) CLIP assays of FLAG-tagged eIF3j using regular S2 cells. RT-qPCR was performed with RNA extracts from CLIP samples to measure the binding of eIF3j to the indicated endogenous ribo-circRNAs. Data were normalized to the negative IgG sample. $^{**}P < 0.01$; $^{*}P < 0.05$. (**B**) CLIP assays of FLAG-tagged eIF3a using regular S2 cells depleted of eIF3j. β-gal dsRNA served as a negative control. RT-qPCR was performed with RNA extracts from CLIP samples to measure the binding of eIF3a to the eIF3j-associated ribo-circRNAs. Data were normalized to the negative IgG sample. $^{**}P < 0.01$; $^{*}P < 0.05$. (**C**) A schematic overview of the construction of the *circPde8* expression vector which is modified from the previously described Hy_pMT laccase2 MCS exon vector. The *circPde8* vector was used to generate a stable cell line using S2 cells for D–H. (**D, E**) Immunofluorescence assays were performed to examine the subcellular localization of CdPde8 in the *circPde8* stable line. Scale bar = 5 μm. The nuclear (Nuc) and cytoplasmic (Cyto) signals of CdPde8 were quantified from 102 cells. (**F–H**) The individual depletion of eIF3a, eIF3b, and eIF3j in the *circPde8* stable cell line. Western blots and RT-qPCR were performed to detect CdPde8 (F, G) and *circPde8* (H), respectively. β-gal dsRNA served as a negative control. The CdPde8 level was quantified from three independent blots. $^{**}P < 0.01$; $^{*}P < 0.05$. All data were generated from three independent biological replicates and are shown as means ± SEM.

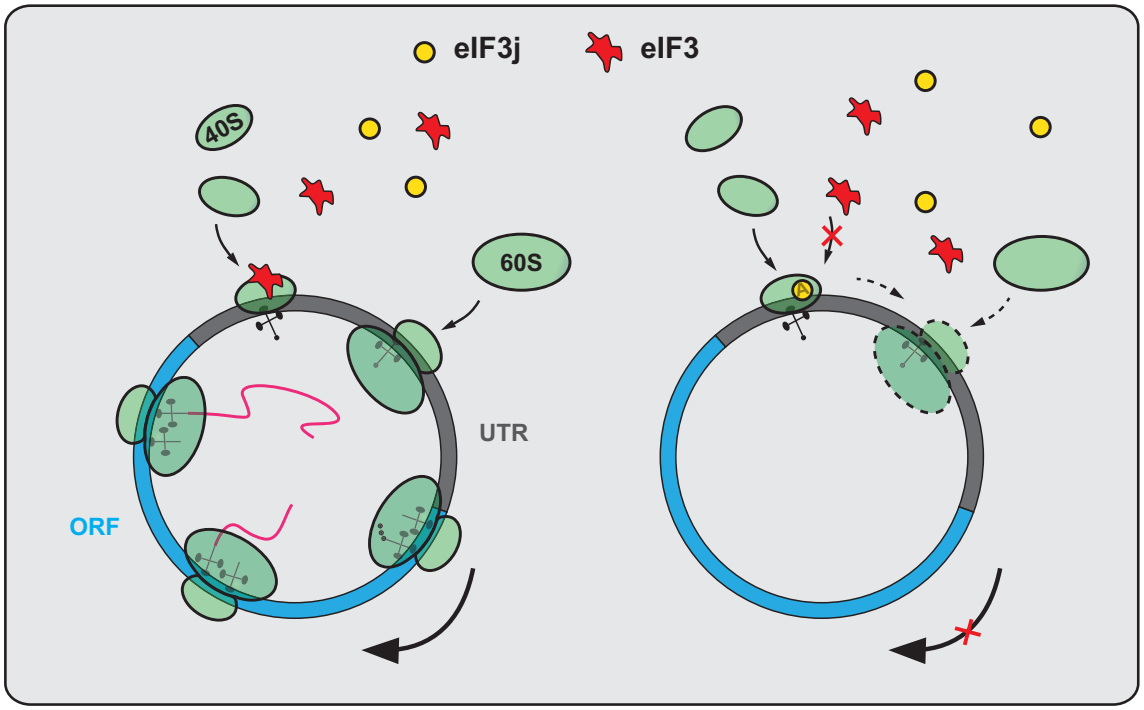

Figure 9. A working model for eIF3j-mediated circRNA translation repression. eIF3j inhibits circRNA translation initiation by blocking the eIF3 complex from binding to translatable circRNAs (possibly in the A site).

dispensable for normal growth and viability of *Caenorhabditis elegans* among all 12 eIF3 subunits (87). The rate of bulk translation initiation is not attenuated in worm mutants lacking eIF3k or eIF3l (87). Moreover, a recent study has demonstrated that eIF3k and eIF3l are non-essential eIF3 subunits with no effect on the integrity of the whole eIF3 complex and are able to antagonize mRNA recruitment to the 43S PIC in human cells (88). As exemplified by *RPL41* mRNA, the individual knockdown of eIF3k and eIF3l significantly promoted the recruitment level of *RPL41* mRNA up to 124–132% (88). Based on these findings, we thus speculate that eIF3k and eIF3l may not be specific for translational control of circRNAs.

eIF2 is a heterotrimeric complex (containing eIF2α, eIF2β, and eIF2γ) used to transfer Met-tRNAi to the 40S ribosomal subunit. The action of eIF2 is generally considered as a rate-limiting step in mRNA translation (51–54). However, we observed that knockdown of eIF2γ (the core of eIF2) and eIF2α had only a limited effect on the translation efficiency of *circSfl* (Figure 2B–D). This indicates that circRNA translation (at least for *circSfl*) may be controlled via an eIF2-independent mechanism. In fact, the eukaryotic translation initiation machinery is able to operate without eIF2 under stressed conditions (55–57). For example, in human cells, the hepatitis C virus (HCV) IRES can make use of a bacterial-like pathway to direct translation and 80S complex formation with the assistance of eIF3 and eIF5B when eIF2 is inactivated by phosphorylation (56). In addition to eIF5B, eIF2A and eIF2D could be other candidates for Met-tRNAi delivery in circRNA translation, since there are studies showing these eIFs can deliver the initiator tRNA into the ribosome under specific contexts (89–91). For example, eIF2A facilitates Met-tRNAi delivery through a direct interaction with a stem-loop structure located in the IRES of c-Src mRNA, which is required for cell growth under stress conditions (89).

eIFs in circRNA biogenesis

Besides circRNA translation, we also identified a subset of eIFs as potent regulators required for *circSfl* biogenesis. For example, the *circSfl* level dropped to ∼16% upon depletion of eIF4A (Figure 2D), an essential subunit of the eIF4F complex. eIF4F comprises the scaffold protein eIF4G, the cap-binding protein eIF4E, and the DEAD-box RNA helicase eIF4A (51–54). Different from eIF4A, knockdown of eIF4E1 and its paralogs only had a marginal effect on *circSfl* biogenesis (Figure 2D). This somehow rules out the possibility that eIF4A indirectly affects *circSfl* biogenesis through controlling the translation of circRNA biogenesis factors. Instead, eIF4A may function via an eIF4F-independent mechanism. Consistent with our hypothesis, an array of studies have demonstrated that eIF4A3 can promote the back-splicing reaction by directly interacting with the flanking sequence of circularizing exons in mammalian cells (92–94). Since several eIFs have been reported as nucleocytoplasmic shuttling proteins (95–97), the nuclear functions of eIFs should be taken into consideration in future.

RNA regulons in circRNA translation

CircRNA lacks the 5′ cap structure utilized by the canonical translation pathway. To data, different RNA elements have been reported to function in the cap-independent transla-

tion of protein-coding circRNAs. For example, the IRES-like regulon, a complex scaffold typically present in the circRNA UTR, is capable of directly recruiting the translation initiation machinery in the absence of the 5′ cap structure and cap-binding protein eIF4E (27,28). In addition, a subset of circRNAs consist of the consensus m^6A motif which is specifically recognized by the m^6A reader YTHDF3. YTHDF3 then recruits eIF4G2 to m^6A-modified circRNAs to initiate their translation (29). Our study is unique in that we revealed that eIF3j negatively regulates *circSfl* translation through a direct interaction with an RNA regulon present in the UTR, further supporting a combination of *cis*- and *trans*-acting regulators in the translational regulation of circRNAs.

Theoretically, exogenous circRNA is an ideal translation tool to generate functional proteins due to its long half-life. However, one fundamental limitation to its broad application is its relatively low translation initiation efficiency in eukaryotic system (27–29). To overcome this obstacle, an array of RNA elements, including IRES and 18S rRNA complementary sequences, are used to engineer circRNAs (98–100). But these inserts also generate some side effects, such as forming unexpected structures with proximal sequences or even distal sequences through long-distance contacts (98,99). Differently, the RNA regulon (nucleotides 101–200 of the *circSfl* UTR) identified in our study has a low potential to form a complex structure (Figure 6G). Use of this RNA regulon may be an alternative strategy to engineer circRNAs for controllable translation without influences on the overall circRNA structure, which is one of our aims currently.

SUPPLEMENTARY DATA

Supplementary Data are available at NAR Online.

ACKNOWLEDGEMENTS

We thank Dr Jeremy E. Wilusz (University of Pennsylvania) for providing useful circRNA expression vectors. We also thank Dr Qin Deng at Analytical and Testing Center of Chongqing University for the assistance with confocal microscopy analyses.

Author contributions: C.H. conceived this project, supervised its execution, and provided the major funding. Z.S., J.L., R.S., Y.J., R.J., S.L. and G.S. performed experiments, analyzed data, or provided the experimental material. C.H. wrote the manuscript with input from the other co-authors.

FUNDING

National Natural Science Foundation of China [32270601, 32070633]; Chongqing Talents Plan for Young Talents [cstc2022ycjh-bgzxm0140]; Fundamental Research Funds for the Central Universities of China [2022CDJXY-004, 2021CDJZYJH-002]; Innovation Support Program for Overseas Returned Scholars of Chongqing, China [cx2019142]. Funding for open access charge: National Natural Science Foundation of China [32270601].

Conflict of interest statement. None declared.

REFERENCES

1. Chen,L.L. (2020) The expanding regulatory mechanisms and cellular functions of circular RNAs. *Nat. Rev. Mol. Cell Biol.*, **21**, 475–490.
2. Kristensen,L.S., Andersen,M.S., Stagsted,L.V.W., Ebbesen,K.K., Hansen,T.B. and Kjems,J. (2019) The biogenesis, biology and characterization of circular RNAs. *Nat. Rev. Genet.*, **20**, 675–691.
3. Xiao,M.S., Ai,Y. and Wilusz,J.E. (2020) Biogenesis and functions of circular RNAs come into focus. *Trends Cell Biol.*, **30**, 226–240.
4. Zhou,M., Xiao,M.S., Li,Z. and Huang,C. (2021) New progresses of circular RNA biology: from nuclear export to degradation. *RNA Biol*, **18**, 1365–1373.
5. Li,Z., Huang,C., Bao,C., Chen,L., Lin,M., Wang,X., Zhong,G., Yu,B., Hu,W., Dai,L. *et al.* (2015) Exon-intron circular RNAs regulate transcription in the nucleus. *Nat. Struct. Mol. Biol.*, **22**, 256–264.
6. Zhang,Y., Zhang,X.O., Chen,T., Xiang,J.F., Yin,Q.F., Xing,Y.H., Zhu,S., Yang,L. and Chen,L.L. (2013) Circular intronic long noncoding RNAs. *Mol. Cell*, **51**, 792–806.
7. Zhang,M., Zhao,K., Xu,X., Yang,Y., Yan,S., Wei,P., Liu,H., Xu,J., Xiao,F., Zhou,H. *et al.* (2018) A peptide encoded by circular form of LINC-PINT suppresses oncogenic transcriptional elongation in glioblastoma. *Nat. Commun.*, **9**, 4475.
8. Lu,Z., Filonov,G.S., Noto,J.J., Schmidt,C.A., Hatkevich,T.L., Wen,Y., Jaffrey,S.R. and Matera,A.G. (2015) Metazoan tRNA introns generate stable circular RNAs in vivo. *RNA*, **21**, 1554–1565.
9. Ashwal-Fluss,R., Meyer,M., Pamudurti,N.R., Ivanov,A., Bartok,O., Hanan,M., Evantal,N., Memczak,S., Rajewsky,N. and Kadener,S. (2014) circRNA biogenesis competes with pre-mRNA splicing. *Mol. Cell*, **56**, 55–66.
10. Liang,D., Tatomer,D.C., Luo,Z., Wu,H., Yang,L., Chen,L.L., Cherry,S. and Wilusz,J.E. (2017) The output of protein-coding genes shifts to circular RNAs when the Pre-mRNA processing machinery is limiting. *Mol. Cell*, **68**, 940–954.
11. Liang,D. and Wilusz,J.E. (2014) Short intronic repeat sequences facilitate circular RNA production. *Genes Dev.*, **28**, 2233–2247.
12. Zhang,X.O., Wang,H.B., Zhang,Y., Lu,X., Chen,L.L. and Yang,L. (2014) Complementary sequence-mediated exon circularization. *Cell*, **159**, 134–147.
13. Carmody,S.R. and Wente,S.R. (2009) mRNA nuclear export at a glance. *J. Cell Sci.*, **122**, 1933–1937.
14. Kohler,A. and Hurt,E. (2007) Exporting RNA from the nucleus to the cytoplasm. *Nat. Rev. Mol. Cell Biol.*, **8**, 761–773.
15. Chen,L., Wang,Y., Lin,J., Song,Z., Wang,Q., Zhao,W., Wang,Y., Xiu,X., Deng,Y., Li,X. *et al.* (2022) Exportin 4 depletion leads to nuclear accumulation of a subset of circular RNAs. *Nat. Commun.*, **13**, 5769.
16. Chen,L., Huang,C. and Shan,G. (2022) Circular RNAs in physiology and non-immunological diseases. *Trends Biochem. Sci*, **47**, 250–264.
17. Li,J., Sun,D., Pu,W., Wang,J. and Peng,Y. (2020) Circular RNAs in cancer: biogenesis, function, and clinical significance. *Trends Cancer*, **6**, 319–336.
18. Yan,L. and Chen,Y.G. (2020) Circular RNAs in immune response and viral infection. *Trends Biochem. Sci*, **45**, 1022–1034.
19. Fischer,J.W. and Leung,A.K. (2017) CircRNAs: a regulator of cellular stress. *Crit. Rev. Biochem. Mol. Biol.*, **52**, 220–233.
20. Chen,X., Zhou,M., Yant,L. and Huang,C. (2022) Circular RNA in disease: basic properties and biomedical relevance. *Wiley Interdiscip. Rev. RNA*, e1723.
21. Gao,L., Chang,S., Xia,W., Wang,X., Zhang,C., Cheng,L., Liu,X., Chen,L., Shi,Q., Huang,J. *et al.* (2020) Circular RNAs from BOULE play conserved roles in protection against stress-induced fertility decline. *Sci. Adv.*, **6**, eabb7426.
22. Bronisz,A., Rooj,A.K., Krawczynski,K., Peruzzi,P., Salinska,E., Nakano,I., Purow,B., Chiocca,E.A. and Godlewski,J. (2020) The nuclear DICER-circular RNA complex drives the deregulation of the glioblastoma cell microRNAome. *Sci. Adv.*, **6**, eabc0221.
23. Conn,V.M., Hugouvieux,V., Nayak,A., Conos,S.A., Capovilla,G., Cildir,G., Jourdain,A., Tergaonkar,V., Schmid,M., Zubieta,C. *et al.* (2017) A circRNA from SEPALLATA3 regulates splicing of its cognate mRNA through R-loop formation. *Nat Plants*, **3**, 17053.
24. Chen,R.X., Chen,X., Xia,L.P., Zhang,J.X., Pan,Z.Z., Ma,X.D., Han,K., Chen,J.W., Judde,J.G., Deas,O. *et al.* (2019)

N(6)-methyladenosine modification of circNSUN2 facilitates cytoplasmic export and stabilizes HMGA2 to promote colorectal liver metastasis. *Nat. Commun.*, **10**, 4695.
25. Wu,F., Han,B., Wu,S., Yang,L., Leng,S., Li,M., Liao,J., Wang,G., Ye,Q., Zhang,Y. *et al.* (2019) Circular RNA TLK1 aggravates neuronal injury and neurological deficits after ischemic stroke via miR-335-3p/TIPARP. *J. Neurosci.*, **39**, 7369–7393.
26. Xu,X., Zhang,J., Tian,Y., Gao,Y., Dong,X., Chen,W., Yuan,X., Yin,W., Xu,J., Chen,K. *et al.* (2020) CircRNA inhibits DNA damage repair by interacting with host gene. *Mol. Cancer*, **19**, 128.
27. Legnini,I., Di Timoteo,G., Rossi,F., Morlando,M., Briganti,F., Sthandier,O., Fatica,A., Santini,T., Andronache,A., Wade,M. *et al.* (2017) Circ-ZNF609 is a circular RNA that can be translated and functions in myogenesis. *Mol. Cell*, **66**, 22–37.
28. Pamudurti,N.R., Bartok,O., Jens,M., Ashwal-Fluss,R., Stottmeister,C., Ruhe,L., Hanan,M., Wyler,E., Perez-Hernandez,D., Ramberger,E. *et al.* (2017) Translation of CircRNAs. *Mol. Cell*, **66**, 9–21.
29. Yang,Y., Fan,X., Mao,M., Song,X., Wu,P., Zhang,Y., Jin,Y., Yang,Y., Chen,L.L., Wang,Y. *et al.* (2017) Extensive translation of circular RNAs driven by N(6)-methyladenosine. *Cell Res.*, **27**, 626–641.
30. Huang,W., Ling,Y., Zhang,S., Xia,Q., Cao,R., Fan,X., Fang,Z., Wang,Z. and Zhang,G. (2021) TransCirc: an interactive database for translatable circular RNAs based on multi-omics evidence. *Nucleic Acids Res.*, **49**, D236–D242.
31. Lei,M., Zheng,G., Ning,Q., Zheng,J. and Dong,D. (2020) Translation and functional roles of circular RNAs in human cancer. *Mol. Cancer*, **19**, 30.
32. Sinha,T., Panigrahi,C., Das,D. and Chandra Panda,A. (2021) Circular RNA translation, a path to hidden proteome. *Wiley Interdiscip. Rev. RNA*, **13**, e1685.
33. Shi,Y., Jia,X. and Xu,J. (2020) The new function of circRNA: translation. *Clin. Transl. Oncol.*, **22**, 2162–2169.
34. Weigelt,C.M., Sehgal,R., Tain,L.S., Cheng,J., Esser,J., Pahl,A., Dieterich,C., Gronke,S. and Partridge,L. (2020) An insulin-sensitive circular RNA that regulates lifespan in drosophila. *Mol. Cell*, **79**, 268–279.
35. Gao,X., Xia,X., Li,F., Zhang,M., Zhou,H., Wu,X., Zhong,J., Zhao,Z., Zhao,K., Liu,D. *et al.* (2021) Circular RNA-encoded oncogenic E-cadherin variant promotes glioblastoma tumorigenicity through activation of EGFR-STAT3 signalling. *Nat. Cell Biol.*, **23**, 278–291.
36. Gomes-Duarte,A., Lacerda,R., Menezes,J. and Romao,L. (2018) eIF3: a factor for human health and disease. *RNA Biol*, **15**, 26–34.
37. Valasek,L.S., Zeman,J., Wagner,S., Beznoskova,P., Pavlikova,Z., Mohammad,M.P., Hronova,V., Herrmannova,A., Hashem,Y. and Gunisova,S. (2017) Embraced by eIF3: structural and functional insights into the roles of eIF3 across the translation cycle. *Nucleic. Acids. Res.*, **45**, 10948–10968.
38. Wolf,D.A., Lin,Y., Duan,H. and Cheng,Y. (2020) eIF-Three to Tango: emerging functions of translation initiation factor eIF3 in protein synthesis and disease. *J. Mol. Cell Biol.*, **12**, 403–409.
39. Lee,A.S., Kranzusch,P.J. and Cate,J.H. (2015) eIF3 targets cell-proliferation messenger RNAs for translational activation or repression. *Nature*, **522**, 111–114.
40. Pulos-Holmes,M.C., Srole,D.N., Juarez,M.G., Lee,A.S., McSwiggen,D.T., Ingolia,N.T. and Cate,J.H. (2019) Repression of ferritin light chain translation by human eIF3. *Elife*, **8**, e48193.
41. Lee,A.S., Kranzusch,P.J., Doudna,J.A. and Cate,J.H. (2016) eIF3d is an mRNA cap-binding protein that is required for specialized translation initiation. *Nature*, **536**, 96–99.
42. Kramer,M.C., Liang,D., Tatomer,D.C., Gold,B., March,Z.M., Cherry,S. and Wilusz,J.E. (2015) Combinatorial control of drosophila circular RNA expression by intronic repeats, hnRNPs, and SR proteins. *Genes Dev.*, **29**, 2168–2182.
43. Huang,C., Liang,D., Tatomer,D.C. and Wilusz,J.E. (2018) A length-dependent evolutionarily conserved pathway controls nuclear export of circular RNAs. *Genes Dev.*, **32**, 639–644.
44. Jia,R., Song,Z., Lin,J., Li,Z., Shan,G. and Huang,C. (2021) Gawky modulates MTF-1-mediated transcription activation and metal discrimination. *Nucleic Acids Res.*, **49**, 6296–6314.
45. Song,Z., Jia,R., Tang,M., Xia,F., Xu,H., Li,Z. and Huang,C. (2021) Antisense oligonucleotide technology can be used to investigate a circular but not linear RNA-mediated function for its encoded gene locus. *Sci. China Life Sci.*, **64**, 784–794.
46. Jia,R., Xiao,M.S., Li,Z., Shan,G. and Huang,C. (2019) Defining an evolutionarily conserved role of GW182 in circular RNA degradation. *Cell Discov.*, **5**, 45.
47. You,J., Song,Z., Lin,J., Jia,R., Xia,F., Li,Z. and Huang,C. (2021) RNAi-directed knockdown induces nascent transcript degradation and premature transcription termination in the nucleus. *Cell Discov.*, **7**, 79.
48. Konig,J., Zarnack,K., Rot,G., Curk,T., Kayikci,M., Zupan,B., Turner,D.J., Luscombe,N.M. and Ule,J. (2010) iCLIP reveals the function of hnRNP particles in splicing at individual nucleotide resolution. *Nat. Struct. Mol. Biol.*, **17**, 909–915.
49. Huang,C., Wang,X., Liu,X., Cao,S. and Shan,G. (2015) RNAi pathway participates in chromosome segregation in mammalian cells. *Cell Discov.*, **1**, 15029.
50. Marygold,S.J., Attrill,H. and Lasko,P. (2017) The translation factors of drosophila melanogaster. *Fly (Austin)*, **11**, 65–74.
51. Borden,K.L.B. and Volpon,L. (2020) The diversity, plasticity, and adaptability of cap-dependent translation initiation and the associated machinery. *RNA Biol.*, **17**, 1239–1251.
52. Hinnebusch,A.G. (2014) The scanning mechanism of eukaryotic translation initiation. *Annu. Rev. Biochem.*, **83**, 779–812.
53. Hinnebusch,A.G. (2017) Structural insights into the mechanism of scanning and start codon recognition in eukaryotic translation initiation. *Trends Biochem. Sci*, **42**, 589–611.
54. Kearse,M.G. and Wilusz,J.E. (2017) Non-AUG translation: a new start for protein synthesis in eukaryotes. *Genes Dev.*, **31**, 1717–1731.
55. Allam,H. and Ali,N. (2010) Initiation factor eIF2-independent mode of c-Src mRNA translation occurs via an internal ribosome entry site. *J. Biol. Chem.*, **285**, 5713–5725.
56. Terenin,I.M., Dmitriev,S.E., Andreev,D.E. and Shatsky,I.N. (2008) Eukaryotic translation initiation machinery can operate in a bacterial-like mode without eIF2. *Nat. Struct. Mol. Biol.*, **15**, 836–841.
57. Pestova,T.V., de Breyne,S., Pisarev,A.V., Abaeva,I.S. and Hellen,C.U. (2008) eIF2-dependent and eIF2-independent modes of initiation on the CSFV IRES: a common role of domain iI. *EMBO J.*, **27**, 1060–1072.
58. Holcik,M. (2015) Could the eIF2alpha-Independent translation be the achilles heel of cancer?*Front. Oncol.*, **5**, 264.
59. Wagner,S., Herrmannova,A., Sikrova,D. and Valasek,L.S. (2016) Human eIF3b and eIF3a serve as the nucleation core for the assembly of eIF3 into two interconnected modules: the yeast-like core and the octamer. *Nucleic Acids Res.*, **44**, 10772–10788.
60. Valasek,L., Nielsen,K.H. and Hinnebusch,A.G. (2002) Direct eIF2-eIF3 contact in the multifactor complex is important for translation initiation in vivo. *EMBO J.*, **21**, 5886–5898.
61. Khoshnevis,S., Gunisova,S., Vlckova,V., Kouba,T., Neumann,P., Beznoskova,P., Ficner,R. and Valasek,L.S. (2014) Structural integrity of the PCI domain of eIF3a/TIF32 is required for mRNA recruitment to the 43S pre-initiation complexes. *Nucleic Acids Res.*, **42**, 4123–4139.
62. Phan,L., Schoenfeld,L.W., Valasek,L., Nielsen,K.H. and Hinnebusch,A.G. (2001) A subcomplex of three eIF3 subunits binds eIF1 and eIF5 and stimulates ribosome binding of mRNA and tRNA(i)Met. *EMBO J.*, **20**, 2954–2965.
63. Simonetti,A., Brito Querido,J., Myasnikov,A.G., Mancera-Martinez,E., Renaud,A., Kuhn,L. and Hashem,Y. (2016) eIF3 peripheral subunits rearrangement after mRNA binding and start-codon recognition. *Mol. Cell*, **63**, 206–217.
64. Bochler,A., Querido,J.B., Prilepskaja,T., Soufari,H., Simonetti,A., Del Cistia,M.L., Kuhn,L., Ribeiro,A.R., Valasek,L.S. and Hashem,Y. (2020) Structural differences in translation initiation between pathogenic trypanosomatids and their mammalian hosts. *Cell Rep.*, **33**, 108534.
65. des Georges,A., Dhote,V., Kuhn,L., Hellen,C.U., Pestova,T.V., Frank,J. and Hashem,Y. (2015) Structure of mammalian eIF3 in the context of the 43S preinitiation complex. *Nature*, **525**, 491–495.
66. Zhou,M., Sandercock,A.M., Fraser,C.S., Ridlova,G., Stephens,E., Schenauer,M.R., Yokoi-Fong,T., Barsky,D., Leary,J.A., Hershey,J.W. *et al.* (2008) Mass spectrometry reveals modularity and a complete subunit interaction map of the eukaryotic translation factor eIF3. *Proc. Natl. Acad. Sci. U.S.A.*, **105**, 18139–18144.

67. Wagner,S., Herrmannova,A., Malik,R., Peclinovska,L. and Valasek,L.S. (2014) Functional and biochemical characterization of human eukaryotic translation initiation factor 3 in living cells. *Mol. Cell. Biol.*, **34**, 3041–3052.
68. Valasek,L., Phan,L., Schoenfeld,L.W., Valaskova,V. and Hinnebusch,A.G. (2001) Related eIF3 subunits TIF32 and HCR1 interact with an RNA recognition motif in PRT1 required for eIF3 integrity and ribosome binding. *EMBO J.*, **20**, 891–904.
69. Fraser,C.S., Berry,K.E., Hershey,J.W. and Doudna,J.A. (2007) eIF3j is located in the decoding center of the human 40S ribosomal subunit. *Mol. Cell*, **26**, 811–819.
70. Jia,R., Lin,J., You,J., Li,S., Shan,G. and Huang,C. (2022) The DEAD-box helicase Hlc regulates basal transcription and chromatin opening of stress-responsive genes. *Nucleic Acids Res.*, **50**, 9175–9189.
71. Bellucci,M., Agostini,F., Masin,M. and Tartaglia,G.G. (2011) Predicting protein associations with long noncoding RNAs. *Nat. Methods*, **8**, 444–445.
72. Elantak,L., Wagner,S., Herrmannova,A., Karaskova,M., Rutkai,E., Lukavsky,P.J. and Valasek,L. (2010) The indispensable N-terminal half of eIF3j/HCR1 cooperates with its structurally conserved binding partner eIF3b/PRT1-RRM and with eIF1A in stringent AUG selection. *J. Mol. Biol.*, **396**, 1097–1116.
73. Fraser,C.S., Lee,J.Y., Mayeur,G.L., Bushell,M., Doudna,J.A. and Hershey,J.W. (2004) The j-subunit of human translation initiation factor eIF3 is required for the stable binding of eIF3 and its subcomplexes to 40 S ribosomal subunits in vitro. *J. Biol. Chem.*, **279**, 8946–8956.
74. Xue,S., Tian,S., Fujii,K., Kladwang,W., Das,R. and Barna,M. (2015) RNA regulons in hox 5' UTRs confer ribosome specificity to gene regulation. *Nature*, **517**, 33–38.
75. Leppek,K., Das,R. and Barna,M. (2018) Functional 5' UTR mRNA structures in eukaryotic translation regulation and how to find them. *Nat. Rev. Mol. Cell Biol.*, **19**, 158–174.
76. Sehgal,A., Briggs,J., Rinehart-Kim,J., Basso,J. and Bos,T.J. (2000) The chicken c-Jun 5' untranslated region directs translation by internal initiation. *Oncogene*, **19**, 2836–2845.
77. Gruber,A.R., Lorenz,R., Bernhart,S.H., Neubock,R. and Hofacker,I.L. (2008) The vienna RNA websuite. *Nucleic Acids Res.*, **36**, W70–W74.
78. Lorenz,R., Bernhart,S.H., Honer Zu Siederdissen,C., Tafer,H., Flamm,C., Stadler,P.F. and Hofacker,I.L. (2011) ViennaRNA package 2.0. *Algorithms Mol. Biol.*, **6**, 26.
79. Westholm,J.O., Miura,P., Olson,S., Shenker,S., Joseph,B., Sanfilippo,P., Celniker,S.E., Graveley,B.R. and Lai,E.C. (2014) Genome-wide analysis of drosophila circular RNAs reveals their structural and sequence properties and age-dependent neural accumulation. *Cell Rep.*, **9**, 1966–1980.
80. Kondo,T., Motoshima,H., Igata,M., Kawashima,J., Matsumura,T., Kai,H. and Araki,E. (2014) The role of heat shock response in insulin resistance and diabetes. *Diabetes Metab J*, **38**, 100–106.
81. Wu,X., Xiao,S., Zhang,M., Yang,L., Zhong,J., Li,B., Li,F., Xia,X., Li,X., Zhou,H. *et al.* (2021) A novel protein encoded by circular SMO RNA is essential for hedgehog signaling activation and glioblastoma tumorigenicity. *Genome Biol.*, **22**, 33.
82. Li,Y., Chen,B., Zhao,J., Li,Q., Chen,S., Guo,T., Li,Y., Lai,H., Chen,Z., Meng,Z. *et al.* (2021) HNRNPL circularizes ARHGAP35 to produce an oncogenic protein. *Adv. Sci. (Weinh)*, **8**, 2001701.
83. Benne,R. and Hershey,J.W. (1978) The mechanism of action of protein synthesis initiation factors from rabbit reticulocytes. *J. Biol. Chem.*, **253**, 3078–3087.
84. Unbehaun,A., Borukhov,S.I., Hellen,C.U. and Pestova,T.V. (2004) Release of initiation factors from 48S complexes during ribosomal subunit joining and the link between establishment of codon-anticodon base-pairing and hydrolysis of eIF2-bound GTP. *Genes Dev.*, **18**, 3078–3093.
85. Aylett,C.H., Boehringer,D., Erzberger,J.P., Schaefer,T. and Ban,N. (2015) Structure of a yeast 40S-eIF1-eIF1A-eIF3-eIF3j initiation complex. *Nat. Struct. Mol. Biol.*, **22**, 269–271.
86. Sokabe,M. and Fraser,C.S. (2014) Human eukaryotic initiation factor 2 (eIF2)-GTP-Met-tRNAi ternary complex and eIF3 stabilize the 43 s preinitiation complex. *J. Biol. Chem.*, **289**, 31827–31836.
87. Cattie,D.J., Richardson,C.E., Reddy,K.C., Ness-Cohn,E.M., Droste,R., Thompson,M.K., Gilbert,W.V. and Kim,D.H. (2016) Mutations in nonessential eIF3k and eIF3l genes confer lifespan extension and enhanced resistance to ER stress in caenorhabditis elegans. *PLoS Genet.*, **12**, e1006326.
88. Herrmannova,A., Prilepskaja,T., Wagner,S., Sikrova,D., Zeman,J., Poncova,K. and Valasek,L.S. (2020) Adapted formaldehyde gradient cross-linking protocol implicates human eIF3d and eIF3c, k and l subunits in the 43S and 48S pre-initiation complex assembly, respectively. *Nucleic. Acids. Res.*, **48**, 1969–1984.
89. Kwon,O.S., An,S., Kim,E., Yu,J., Hong,K.Y., Lee,J.S. and Jang,S.K. (2017) An mRNA-specific tRNAi carrier eIF2A plays a pivotal role in cell proliferation under stress conditions: stress-resistant translation of c-Src mRNA is mediated by eIF2A. *Nucleic Acids Res.*, **45**, 296–310.
90. Skabkin,M.A., Skabkina,O.V., Dhote,V., Komar,A.A., Hellen,C.U. and Pestova,T.V. (2010) Activities of ligatin and MCT-1/DENR in eukaryotic translation initiation and ribosomal recycling. *Genes Dev.*, **24**, 1787–1801.
91. Dmitriev,S.E., Terenin,I.M., Andreev,D.E., Ivanov,P.A., Dunaevsky,J.E., Merrick,W.C. and Shatsky,I.N. (2010) GTP-independent tRNA delivery to the ribosomal P-site by a novel eukaryotic translation factor. *J. Biol. Chem.*, **285**, 26779–26787.
92. Feng,Z.H., Zheng,L., Yao,T., Tao,S.Y., Wei,X.A., Zheng,Z.Y., Zheng,B.J., Zhang,X.Y., Huang,B., Liu,J.H. *et al.* (2021) EIF4A3-induced circular RNA PRKAR1B promotes osteosarcoma progression by miR-361-3p-mediated induction of FZD4 expression. *Cell Death. Dis.*, **12**, 1025.
93. Wang,R., Zhang,S., Chen,X., Li,N., Li,J., Jia,R., Pan,Y. and Liang,H. (2018) EIF4A3-induced circular RNA MMP9 (circMMP9) acts as a sponge of miR-124 and promotes glioblastoma multiforme cell tumorigenesis. *Mol. Cancer*, **17**, 166.
94. Zheng,X., Huang,M., Xing,L., Yang,R., Wang,X., Jiang,R., Zhang,L. and Chen,J. (2020) The circRNA circSEPT9 mediated by E2F1 and EIF4A3 facilitates the carcinogenesis and development of triple-negative breast cancer. *Mol. Cancer*, **19**, 73.
95. Salton,G.D., Laurino,C., Mega,N.O., Delgado-Canedo,A., Setterblad,N., Carmagnat,M., Xavier,R.M., Cirne-Lima,E., Lenz,G., Henriques,J.A.P. *et al.* (2017) Deletion of eIF2beta lysine stretches creates a dominant negative that affects the translation and proliferation in human cell line: a tool for arresting the cell growth. *Cancer Biol. Ther.*, **18**, 560–570.
96. Osborne,M.J. and Borden,K.L. (2015) The eukaryotic translation initiation factor eIF4E in the nucleus: taking the road less traveled. *Immunol. Rev.*, **263**, 210–223.
97. Chan,C.C., Dostie,J., Diem,M.D., Feng,W., Mann,M., Rappsilber,J. and Dreyfuss,G. (2004) eIF4A3 is a novel component of the exon junction complex. *RNA*, **10**, 200–209.
98. Wesselhoeft,R.A., Kowalski,P.S. and Anderson,D.G. (2018) Engineering circular RNA for potent and stable translation in eukaryotic cells. *Nat. Commun.*, **9**, 2629.
99. Chen,C.K., Cheng,R., Demeter,J., Chen,J., Weingarten-Gabbay,S., Jiang,L., Snyder,M.P., Weissman,J.S., Segal,E., Jackson,P.K. *et al.* (2021) Structured elements drive extensive circular RNA translation. *Mol. Cell*, **81**, 4300–4318.
100. Fan,X., Yang,Y., Chen,C. and Wang,Z. (2022) Pervasive translation of circular RNAs driven by short IRES-like elements. *Nat. Commun.*, **13**, 3751.